

A study on Vortex Induced Vibrations Suppression Devices for Marine Pipeline

Authors: Shivanand, Abhijeet Sajjan

ABSTRACT

Vortex induced vibration is caused due to the periodic shedding of vortices from either sides due to flow separation over a bluff body. An asymmetrical flow pattern develops around the body due to the periodic shedding of vortices and changes the pressure distribution on the surface of the body which creates fluctuating lift forces on either side of the body, thus making the structure to vibrate. The frequency of shedding depends on diameter of the body and the velocity of flow (Reynolds Number). High amplitudes of vibrations can occur when the frequency of vortex shedding coincides with the natural frequency of the structure. Vortex induced vibrations (VIV) are an important source for fatiguedamage of the structures. This phenomenon can typically occur on long chimneys, cables used in bridges, power transmission lines in air. In marine environment the structures subjected to these vibrations are marine risers, anchor lines and free spanning pipelines etc. Large diameter pipes used to draw cold water from deeper water depths could be susceptible to vortex induced vibrations. Currently NIOT is working on a bundle of pipes forming a conduit. Each pipe is made of High-density Polyethylene (HDPE). The bundles with 2 and 3 cylinders are considered for the study. The flow around these pipes will be studied by performing CFD analysis considering the cylinders to be stationary. The present work is focused on studying flow behaviour around the pipes, vortex shedding around cylinders using Ansys Fluent.

KEYWORDS: Vortex Induced Vibration (VIV); Computational Fluid Dynamics (CFD); Ansys Fluent.

CHAPTER 1

INTRODUCTION

1.1 General

Vortex-shedding is a phenomenon that occurs over bluff bodies subjected to sustained currents, which might result in large transverse motions (Humphries and Walker 1987). When a flowing medium strikes a non-streamlined bluff object, it moves around the object generating alternating pressure forces on either side of the bluff body. This results in the formation of vortices, causing periodic forces, which are strong enough to set the body into oscillatory motion. Vortex-Induced Vibration (VIV) are the outcome of such exciting forces that are generated by vortex-shedding on hull of a bluff body, causing response closer to the resonant period (Anagnostopoulos and Bearman 1992; Bearman 1984). Experimental investigations carried out on elastically mounted cylinder showed wake formation with the maximum amplitude occurring near lower limit of lock-in region. Due to VIV, structure undergoes a number of stress cycles leading to fatigue damage. Based upon the

significant consequences of VIV on several mechanical systems and ocean engineering structures, VIV suppression configurations are encouraged (Sarpkaya 1978). Observation of large amplitude responses of systems that used water as working fluid necessitates the importance of VIV suppression by design (Khalak and Williamson 1991; Zdravkovich 1981). While several suppression techniques of VIV suppression are successfully developed, cost and difficulty of implementation restricted their applications (Owen and Masa 2003). In view of suppressing VIV, use of helical strakes proved to be effective in strengthening the cylinder to resist larger bending moments that result from the increased drag. Under close examination of flow behind a pair of cylinders, pair of anti-phase streets and in-phase shedding can cause the formation of a single wake in large scale (Govardhan and Williamson 2000; Brika and Laneville 1993). Their applications in marine risers by modelling them, as flexible cylinders are quite successful. 398 7 Applications in Preliminary Analysis and Design Normalized vortex-shedding frequency, which is represented by Strouhal number is affected by various flow velocities (Lesage and Garthshore 1987). An application example on experimental investigations of a rigid cylinder, resembling hull of a Spar platform is presented. Flow around a cylinder is one of the classical topics in field of hydrodynamics (Mutlu and Jorgen 2003). Models proposed by several researchers consider rigid circular cylinder with a single degree of freedom in the cross-flow direction (Gabbai and Benaroya 2005; Rodolfo et al. 2011). Experimental investigations carried out on long, flexible cylinders indicated the formation of vortex-induced motion in the form of hysteresis loop motion in which contributions are seen from each of the vortex-shedding modes (Chandrasekaran and Marin 2016). Amongst various methods proposed to suppress VIV, strakes and shrouds are found to be effective regardless the orientation of structure to waves and current; but showed a substantial increase in drag, resulting in high drift. When strakes or bumps are fixed, no regular shedding is observed on the wake side of the cylinder, while major advantage is effective suppression of amplitude of vibration of the cylinder. Recent studies also show the possibilities of suppression of vibration of multiple cylinders using rough strip (Blevins 1994). A few analytical and numerical investigations of VIV on cylinders with low mass and aspect ratio are helpful in modelling wake oscillations and force decomposition, resulting from VIV suppression systems. Alternatively, force reduction is also achieved by providing an outer perforated cover, which alters fluid flow around cylinders in flow regime.

1.2 Objective of the Study

- To study on the Vortex Suppression Devices for marine Pipelines.

1.3 Scope of the Study

- To study the flow behavior around a bare cylinder for different current speeds using CFD.
- To study the flow behavior around a cylinder with different vortex suppression devices (VSD) for different current speeds using CFD.
- Analysis of flow around a cylinder with optimized VSD for different current speeds.

1.4 Literature Review

1. Meghanadhan C A and Sunil A S (2016) worked on study of Vortex Shedding Behind a Bluff Body in a Water Channel. They conducted experiment in water channel installed in fluid mechanics lab to study the flow characteristics and flow pattern in the wake region of a circular cylinder and understand the relation between the Reynolds number and Strouhal number. They found that there was no vortex shedding at $Re=40$. And by the experiment they concluded that the cylinder with helical stakes was the effective device for suppression of vortex induced vibrations as passive control. And also, frequency of vortex shedding was reduced by helical stakes of suitable pitch and height.
2. Alok Mishra and Ashoke de studied on suppression of vortex shedding using slit through a circular cylinder at a low Reynolds number. They performed 2-D simulations on bare cylinder and cylinder with a slit along with the incoming flow. The investigation was done for different slit ratios ($S/D= 0$ to 0.25) at different Re values ($Re= 100$ to 500) to find the slit angle (θ) on vortex shedding. The $S/D=0.25$ at $Re=500$ with Slit angle ($\theta=20^\circ$) illustrates the maximum suppression in vortex shedding.
3. Zheng-Shou Chen and Wu-Joan Kim (2010) have done a Numerical investigation of vortex shedding and vortex-induced vibration for flexible riser models. They used ANSYS MFX solver to solve the two-way FSI problems related to VIV of flexible riser system. They carried out simulations for two flexible riser model systems, one was related to the simulation of vortex visualization in the wake for a riser model subject to forced oscillation, and another was related to the simulation of fluid-structure interaction between the pipes of coupled multi-assembled riser system. The riser model was made of PVC pipes with an outer diameter of 50mm and a wall thickness of 2.5mm. By the study they concluded that in the multi-assembled pipe systems, the external current velocity and the distance between two pipes are the critical factors to determine the vibration state and the steady vibration state in quad-pipe system may be destroyed more easily than dual-pipe system.
4. Dwi Priyanta and Anang Abdullah carried out Analysis of the Suppression Device as Vortex Induced Vibration (VIV) Reducer on Free Span using Finite Element Method. In this study they have used two types of Suppression device i.e., Helical strike and fairing to compared in reduce the impact of VIV. They have done fatigue life calculation for the happening VIV process simulation of Finite Element Method (FEM) using software Ansys Fluent. They concluded that assumed operational designed time of the pipe for 50 years, by the test they found that on the condition of the critical free span exposed VIV the life time value on plain pipe 44.21 years, at and Fairing pipe with 53.09 years and on the pipe with the Helical 52.95 strike year.
5. T. Zhou, S.F. Mohd. Razali, Z. Hao, L. Chenga studied on the study of vortex-induced vibration of a cylinder with helical stakes. They used 80mm cylinder and helical stakes of dimensions of $10d$ in pitch and $0.12d$ in height. It was tested in a wind tunnel and they found that the helical stakes can reduce VIV by about 98%.

6. Satya Prakash Singh, Goutam Biswas, Perumal Nithiarasu have done a numerical study of vortex shedding from a circular cylinder vibrating in the in-line direction. In this study a circular cylinder, vibrating in the in-line direction is placed in a fluid stream and assumed forced vibration as sinusoidal and considered distance between the mean centre of the cylinder and upstream and downstream boundaries are, respectively, 10D and 67.5D, where D is the diameter of the cylinder. They observed that the drag and lift coefficients were perfectly periodic at a Reynolds number of 200 and they reach a chaotic pattern as the Reynolds number is increased to a value of 350.

7. Nur Ain Shafiza Ramzi, Lee Kee Quen, Hidetaka Senga, Hooi-Siang Kang, Meng Hee Lim, Noor Idora Mohd Sukarnoor these all people studied on Suppression of vortex-induced vibration of a rigid cylinder using flexible shrouding. They conducted experimental investigations to find the reduction of VIV and mean drag coefficient (C_d mean) acting on the oscillating cylinder fitted with a shroud of various parameters. By the study they observed that the shroud with mesh size $B = 0.2D$ and mesh thickness $H = 0.03D$ achieved an optimum condition where it was able to suppress the amplitude without increasing C_d mean, with 76.62% of amplitude reduction and 48.40% of C_d mean reduction.

CHAPTER 2

THEORETICAL BACKGROUND

2.1 General

In this chapter, the theoretical fluid behaviour around cylinder is included. The details of software tool ANSYS FLUENT are also included. A brief description about the graphical user interface of the software tool is given. The details of various turbulence models available with ANSYS FLUENT software are included.

2.2 VIV Theory

When a structure, in this case, a spar platform is subjected to the fluid flow, somehow the spar might experience excitations or vibrations. These vibrations known as the flow induced vibrations can lead to the fatigue damage to the structure. Hence, it is essential to take these vibrations into consideration whilst designing structures, particularly cylindrical structures.

2.2.1 Regime of flow

One of the non-dimensionless hydrodynamic numbers that is used to describe the flow around a smooth cylinder is the Reynolds number (Re). By the definition, the Reynolds number is the ratio of the inertia forces to viscous forces and formulated as

$$Re = \frac{UD}{\gamma} \quad (2.1)$$

Where D is the diameter of cylinder, U is the flow velocity and γ is the kinematic viscosity of the fluid. Flow regimes are obtained as the result of tremendous changes of the Reynolds number. The changes of the Reynolds number create separation flows in the wake region of the cylinder, which are called vortices. At low values of Re ($Re < 5$), there no separation occurs. When the Re is further increased, the separation starts to occur and becomes unstable and initiates the phenomenon called vortex shedding at certain frequency. As the result, the wake has an appearance of a vortex street as can be seen in Table 2.1










a)		No separation. Creeping flow	$Re < 5$
b)		A fixed pair of symmetric vortices	$5 < Re < 40$
c)		Laminar vortex street	$40 < Re < 200$
d)		Transition to turbulence in the wake	$200 < Re < 300$
e)		Wake completely turbulent. A: Laminar boundary layer separation	$300 < Re < 3 \times 10^5$ Subcritical
f)		A: Laminar boundary layer separation B: Turbulent boundary layer separation; but boundary layer laminar	$3 \times 10^5 < Re < 3.5 \times 10^5$ Critical (Lower transition)
g)		B: Turbulent boundary layer separation; the boundary layer partly laminar partly turbulent	$3.5 \times 10^5 < Re < 1.5 \times 10^6$ Supercritical
h)		C: Boundary layer comple- tely turbulent at one side	$1.5 \times 10^6 < Re < 4 \times 10^6$ Upper transition
i)		C: Boundary layer comple- tely turbulent at two sides	$4 \times 10^6 < Re$ Transcritical

Figure 2.1 Flow regime around smooth circular cylinder in steady current. (sumer, 2006)

2.2.2 Vortex Shedding

The vortex shedding phenomenon appears when pairs of stable vortices are exposed to small disturbances and become unstable at Re greater than 40. For these values of Re , the boundary layer over the cylinder surface will separate due to the adverse pressure gradient imposed by the divergent geometry of the flow environment at the rear side of the cylinder. As mentioned in the previous section, vortex shedding occurs at a certain frequency, which is called as vortex shedding frequency (f_v). This frequency normalized with the flow velocity U and the

cylinder diameter D , can basically be seen as a function of the Reynolds number. Furthermore, the normalized vortex-shedding frequency is called Strouhal number (St), and formulated as:

$$St = \frac{fvD}{U} \tag{2.2}$$

The relationship between Re and St can be shown in Figure 2.2

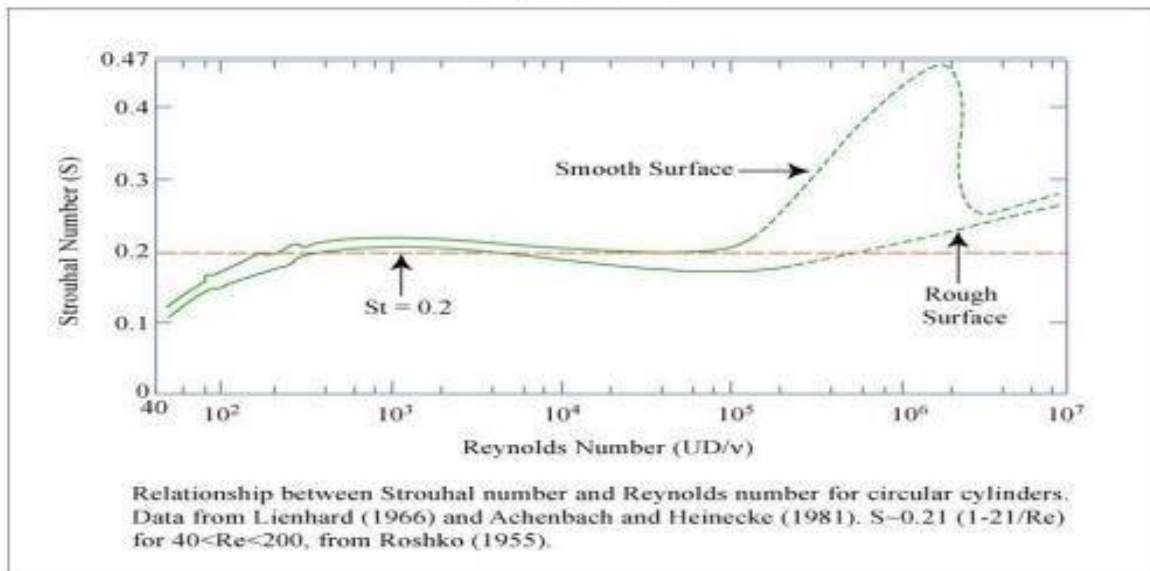


Figure 2.2 Strouhal number for smooth and rough circular cylinder (Linhard, 1966)

The large increase in St at the supercritical region is caused by the delay of the boundary separation. It is known that the separation point of the subcritical regime is different from that of the supercritical regime as shown in Figure 2.2. At the supercritical flow regime, the boundary layers on both sides of the cylinder are turbulent at the separation point. Consequently, the boundary layer separation is delayed since the separation point moves downstream. At this point, the vortices are close to each other and create faster rate than the rate in the subcritical regime, thereby leading to higher values of the Strouhal number.

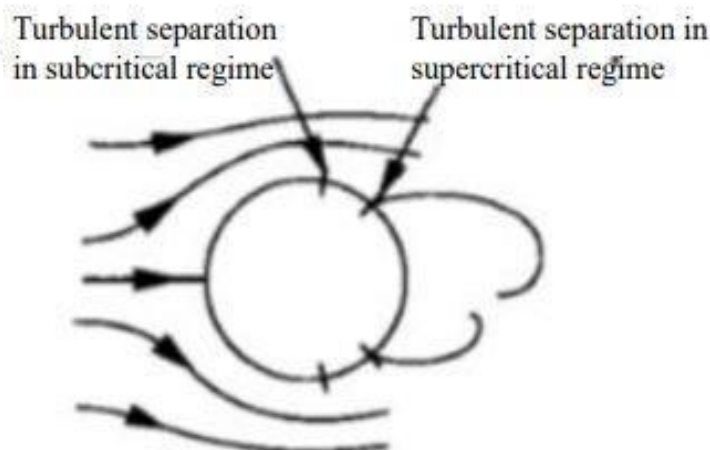


Figure 2.3 Separation point of the subcritical regime and supercritical regime.

When Re reaches the value of 1.5×10^6 , the boundary layer completely becomes turbulent at one side and laminar at the other side. This asymmetric situation is called the lee-wake vortices. What happens next is that lee-wake vortices inhibit the interaction of these vortices, resulting in an irregular and disorderly vortex shedding. When Re is increased to values larger than 4.5×10^6 (transcritical regime), the regular vortex shedding is re-established and St takes the values of $0.25 - 0.30$.

2.2.3 Drag and Lift Forces

As the result of the periodic change of the vortex shedding, the pressure distribution of the cylinder due to the flow will also change periodically, thereby generating a periodic variation in the force components on the cylinder. The force components can be divided into crossflow and in-line directions. The force of the crossflow direction is commonly named as the lift force (F_L) while the latter is named as the drag force (F_D). The lift force appears when the vortex shedding starts to occur and it fluctuates at the vortex shedding frequency. Similarly, the drag force also has the oscillating part due to the vortex shedding, but in addition it also has a force as a result of friction and pressure difference; this part is called the mean drag. Both of the lift and drag forces are formulated as follows:

$$F_L = \hat{F}_L \sin(\omega_s t + \varphi_s) \tag{2.3}$$

$$F_D = F_D \sin(2\omega_s t + \varphi_s) \tag{2.4}$$

F_L and F_D are the amplitudes of the oscillating lift and drag respectively and is the mean drag. It should be noted that drag force oscillated with twice the frequency of oscillation of lift force.

2.2.4 Vortex Induced Motions

Whenever any offshore component like spar hull, pipe, risers are open to a steady current, vortices and alternating eddies will be formed. A vortex forms in the re-circulation to equalise pressure. Disturbances in the flow causes the vortex to be shed, creating a new vortex to equalise the pressure from the preceding vortex. These vortices shed at a regular interval of period. This phenomenon is referred to as vortex shedding. Vortex shedding is an effect of Viscosity and Reynolds number. Reynolds number is a dimensionless quantity which relates which relates inertial forces to the viscous forces in the flow and is given by

$$\bar{R}_e = \frac{\rho u D}{\mu} \tag{2.5}$$

Where, ρ is the density, u is the velocity, D is the diameter and μ is the dynamic viscosity.

At low Reynolds number, viscous forces dominate the flow while at high Reynolds number, inertial forces dominate. The vortex shedding frequency f_s , which is also called as Strouhal frequency is related to a non-dimensional Strouhal number, S

$$f_s = \frac{S V_c}{D} \tag{2.6}$$

Where, V_c is current velocity and D diameter of cylinder.

Strouhal shedding period is defined as the inverse of the Strouhal shedding frequency.

$$T_s = \frac{1}{f_s} \quad (2.7)$$

Natural frequency of structure f_n ,

$$f_n = \frac{1}{2\pi} \sqrt{\frac{K}{M+Ma}} \quad (2.8)$$

$$T_n = \frac{1}{f_n} \quad (2.9)$$

Where, K is lateral stiffness, M is Mass and Ma is added mass of the floating conduit.

Lock-in phenomena is the tendency of the natural period of the structure to match or to synchronize with the shedding period of the structure, where the cylinder will try to lock-in to the frequency shed by the vortices.

$$s = 0.198 \left(1 - \frac{19.7}{ReD}\right) \quad (2.10)$$

The Strouhal number of a static pipe or a cylinder is a function of Reynolds number, but it is less dependent on the surface roughness of the body and the turbulence of the free stream. In the Reynolds number range $250 < Re < 2 \times 10^5$ the empirical formula can be used.

2.2.5 Reduced velocity

When a structure starts to vibrate due to VIV, the reduced velocity becomes useful. The reduced velocity gives information in which velocity ranges VIV will be maximum. It has been seen that the vibration amplitude reaches maximum for reduced velocities which are in the “lock-in” range. For

subcritical flow lock-in occurs at reduced velocities $U_r = 5$ to 7 approximately. Reduced velocity can be divided into two types, true reduced velocity U_r true and nominal reduced velocity U_r nom. The true reduced velocity is based on the frequency at which the cylinder is actually vibrating whilst the nominal reduced velocity is based on the nominal natural frequency, e.g., natural frequency in still water. Reduced velocity is formulated as follows.

$$U_r = \frac{U}{f_n D} \quad (2.11)$$

CHAPTER 3

CFD AND NUMERICAL STUDY

3.1 General

The details of software tool ANSYS FLUENT are also included. A brief description about the graphical user interface of the software tool is given. The details of various turbulence models available with ANSYS FLUENT software are included. Methodology used such as geometric modelling, meshing, physics modelling, solver set up and stopping criteria is explained here.

3.2 Computational Fluid Dynamics

Computational fluid dynamics, usually abbreviated as CFD, is a computer-based simulation or numerical modelling of fluid mechanics to solve and model problems related to fluid flows, heat transfer and associated phenomena such as chemical reactions. CFD provides wide range application for many industrial and non-industrial areas. CFD is a very powerful technique regarding the simulation of fluid flows.

The application of CFD began in 1960's when the aerospace industry has integrated CFD technique into the design, R & D and manufacturing of aircrafts and jet engines. CFD codes are being accepted as design tools by many industrial users. Today, many industrials, for instance, ship industry, power plant, machinery, electronic engineering, chemical process, marine engineering and environmental engineering use CFD as a one of the best design tools. Unlike the model testing facility or experimental laboratory, in CFD simulations there is no need for a big facility. Furthermore, CFD also offers no capacity limit, no model scale limit and cost and cost and schedule efficiency. Indeed, the advantages by using CFD compared to experimental-based approaches can be concluded as follows:

- a. Ability to assess a system that controls experiments is difficult or impossible to perform (very large system).
- b. Ability to assess a system under hazardous conditions (e.g., safety study and accident investigation).
- c. Gives unlimited level of results.

This article describes basic theories and information of fluid dynamics and CFD. Given theories and information are delivered in brief and general. More details of these can be found out at related sources. **FLUID THEORY**

As mentioned in previous section, CFD is the science of predicting fluid flow, heat and mass transfer, chemical reactions, and other related phenomena. The CFD problems are stated in a set of mathematical equations and are solved numerically. These set of mathematical equations are based on the conservation laws of fluid motion, which are conservation of mass, conservation of momentum, conservation of energy etc. For CFD related to fluid flow, the set of mathematical equations are based on conservation of mass and momentum.

Conservation of mass

The mass conservation theory states that the mass will remain constant over time in a closed system. This means that the quantity of mass will not change and, the quantity is conserved.

The mass conservation equation, also called the continuity equation can be written as:

$$\frac{\partial \rho}{\partial t} + \frac{\partial(\rho u)}{\partial x} + \frac{\partial(\rho v)}{\partial y} + \frac{\partial(\rho w)}{\partial z} = S_m \quad (3.1)$$

Equation (3.1) is the general form of the mass conservation equation and is valid for incompressible as well as compressible flows. The source S_m is the mass added to the system and any user-defined sources. The density of the fluid is ρ and the flow of mass in x, y and z direction is u, v and w.

Conservation of momentum.

The conservation of momentum is originally expressed in Newton's second law. Like the velocity, momentum is a vector quantity as well as a magnitude. Momentum is also a conserved quality, meaning that for a closed system, the total momentum will not change if there is no external force.

The momentum conservation equation also known as Navier-Stokes equation in general vector form can be written as:

$$\rho \left(\frac{\partial \bar{v}}{\partial t} + (\bar{v} \cdot \nabla) \bar{v} \right) = -\nabla p + \nabla^2 \bar{v} + \rho f \quad (3.2)$$

3.3 ANSYS FLUENT

ANSYS FLUENT delivers a powerful CFD tool in an easy-to-use environment. ANSYS FLUENT is based on object-oriented programming technology. It is designed to handle large models quickly and efficiently using a unique client-server architecture that seamlessly meshes and simultaneously solves and post-processes over multiple computing resources without requiring additional effort from the user. Much more than just a CFD solver, ANSYS FLUENT is an entire engineering process for solving problems involving flow (of fluids or solids), heat transfer, and stress. The software uses a finite volume approach to solve the problems involving flow of fluids.

3.3.1 GENERAL WORKFLOW OF ANSYS FLUENT

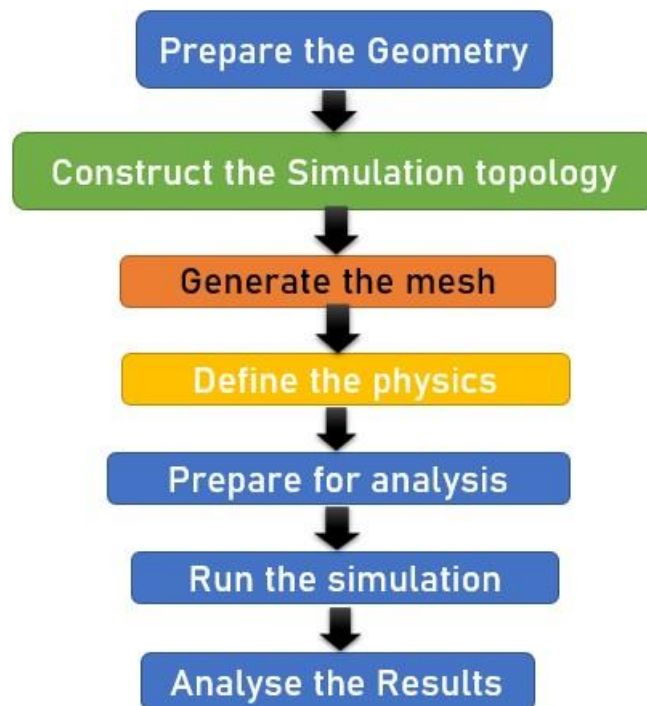


Figure 3.1 General workflow of ANSYS FLUENT

A workflow is the sequence of operations you must work through in order to achieve a certain result.

3.3.2 TURBULENCE MODELS

Turbulent flow can be defined as a chaotic, fluctuating and randomly condition of flow, i.e. velocity fields. These fluctuations mix transported quantities such as momentum, energy, and species concentration, and cause the transported quantities to fluctuate as well. Turbulence is a time-dependent process. Three basic approaches to modelling turbulence are available in Ansys Fluent. These are DNS (direct numerical solution), RANS (Reynolds averaged Navier-Stokes), and LES (large eddy simulation).

Reynolds Averaged Navier-Stokes (RANS)

RANS equations are the time-averaged equations of motion of fluid flow. They govern the transport of the averaged flow quantities, with the complete range of the turbulent scales being modelled. Therefore, it greatly reduces the required computational effort and resources and is widely adopted for practical engineering applications. To obtain the Reynolds-Averaged Navier-Stokes (RANS) equations, the Navier-Stokes equations for the instantaneous velocity and pressure fields are decomposed into a mean value and a fluctuating component. The averaging process may be thought of as time averaging for steady-state situations and ensemble averaging for repeatable transient situations. The resulting equations for the mean quantities are essentially identical to the original equations, except that an additional term now appears in the momentum transport equation. This additional term is a tensor quantity, known as the Reynolds stress tensor, which has the following definition.

$$T_t \equiv -\rho \overline{v'v'} = -\rho \begin{bmatrix} \overline{u'u'} & \overline{u'v'} & \overline{u'w'} \\ \overline{u'v'} & \overline{v'v'} & \overline{v'w'} \\ \overline{u'w'} & \overline{v'w'} & \overline{w'w'} \end{bmatrix} \quad (3.3)$$

To model the Reynolds stress tensor of above equation in terms of the mean flow quantities, and hence provide closure of the governing equations, two basic approaches are used in ANSYS FLUENT:

Eddy viscosity models

Eddy viscosity models use the concept of a turbulent viscosity to model the Reynolds stress tensor as a function of mean flow quantities. The most common model is known as the Boussinesq approximation:

$$T_t = 2\mu_t S - \frac{2}{3}(\mu_t \nabla \cdot v + \rho K)I \quad (3.4)$$

where **S** is the strain tensor

$$S = \frac{1}{2}(\nabla v + \nabla v^T) \quad (3.5)$$

And **K** is the turbulent kinetic energy, μ_t is the turbulent viscosity.

The eddy viscosity models in ANSYS FLUENT solve additional transport equations for scalar quantities that enable the turbulent viscosity to be derived. These include Spalart-Allmaras, K-Epsilon and K-Omega models.

Reynolds Stress Transport Model

Reynolds stress transport models, also known as second-moment closure models, solve transport equations are solved for each component of the Reynolds stress tensor.

K-Epsilon models provide a good compromise between robustness, computational cost and accuracy. They are generally well suited to industrial-type applications that contain complex recirculation, with or without heat transfer.

K-Omega models are similar to K-Epsilon models in that two transport equations are solved but differ in the choice of the second transported turbulence variable. The performance differences are likely to be a result of the subtle differences in the models, rather than a higher degree of complexity in the physics being captured. These models have seen most application in the aerospace industry. Therefore, they are recommended as an alternative to the Spalart-Allmaras models for similar types of applications.

3.3.3 METHODOLOGY OF CFD

In general, CFD simulations can be distinguished into three main stages, which are;

- 1) pre-processor
- 2) simulator or solver and
- 3) post-processor

TRIAL DONE FOR VORTEX SHEDDING

1. Pre-Processor

The pre-processing stage includes:

- Solution domain defining. The solution domain defines the abstract environment where the solution is calculated. The shape of the solution domain can be circular or rectangular. Generally, many simulations use a rectangular box shape as the solution domain as shown in the figure.

The choice of solution domain shape and size can affect the solution of the problem. The smaller sized of domains need less iterations to solve the problem, in contrast to big domains, which need more time to find the solution.

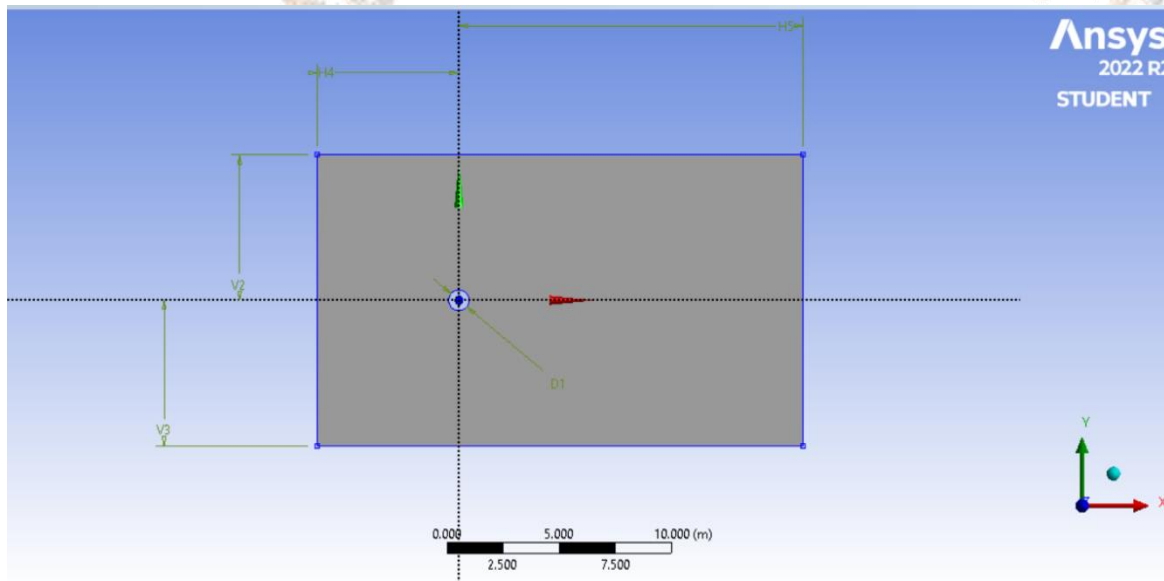


Fig. 3.2: Domain condition of the cylinder

D1	0.90 m
V2	6.3 m
V3	6.3 m
H4	6.3 m
H5	15.3 m

Table no 1.: Dimensions of the Domain

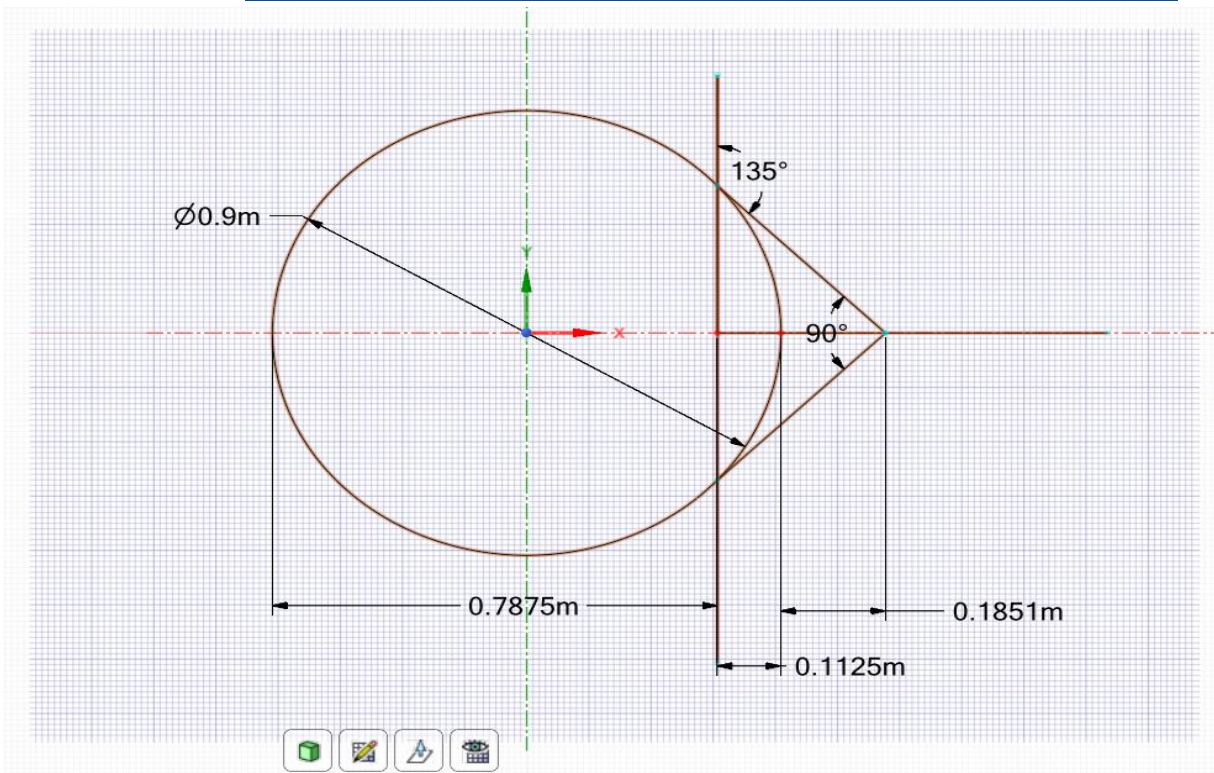


Fig 3.3.: Cylinder with fixed fairing of 0.125D

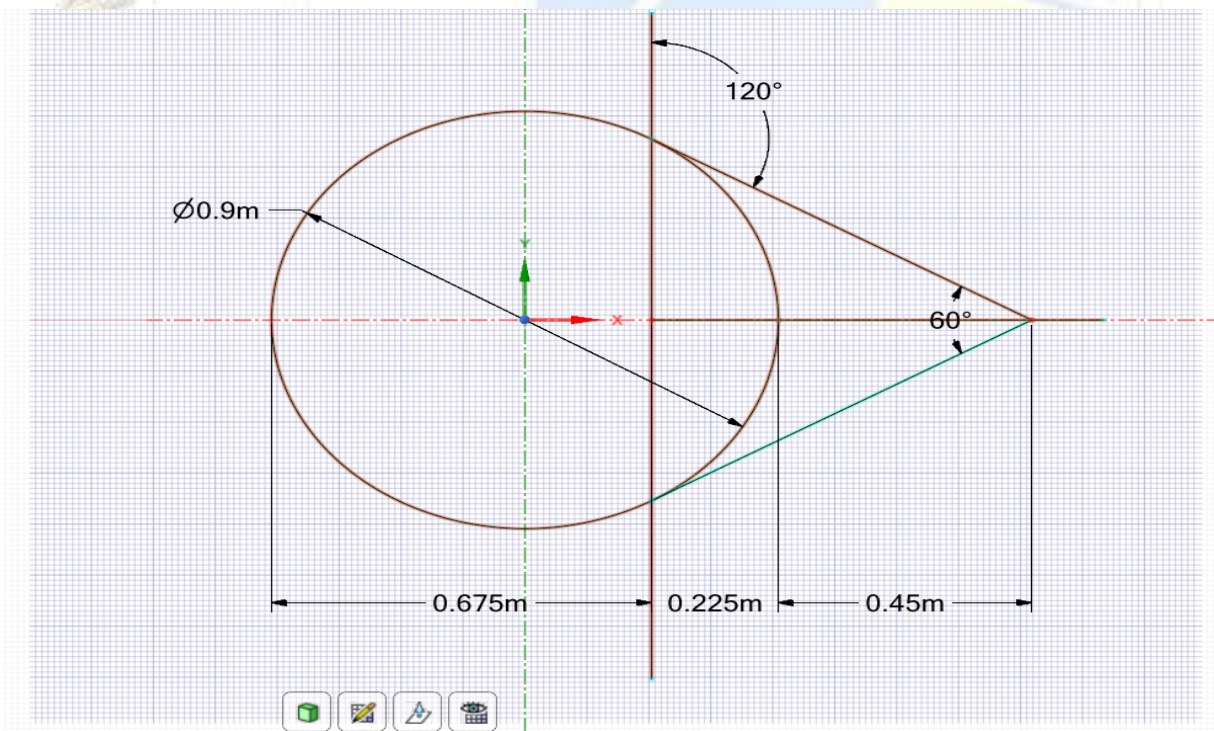


Fig 3.4: Cylinder fixed with fairing 0.25D

• **Mesh generation**

After the solution domain has been defined, we shall generate the mesh within the solution domain. The term mesh generation and grid generation is often interchangeable. The mesh or grid is defined as the discrete locations at which the variables are to be calculated and to be solved. The grid divides the solution domain into a finite number of sub domains, for instance elements, control volumes etc.

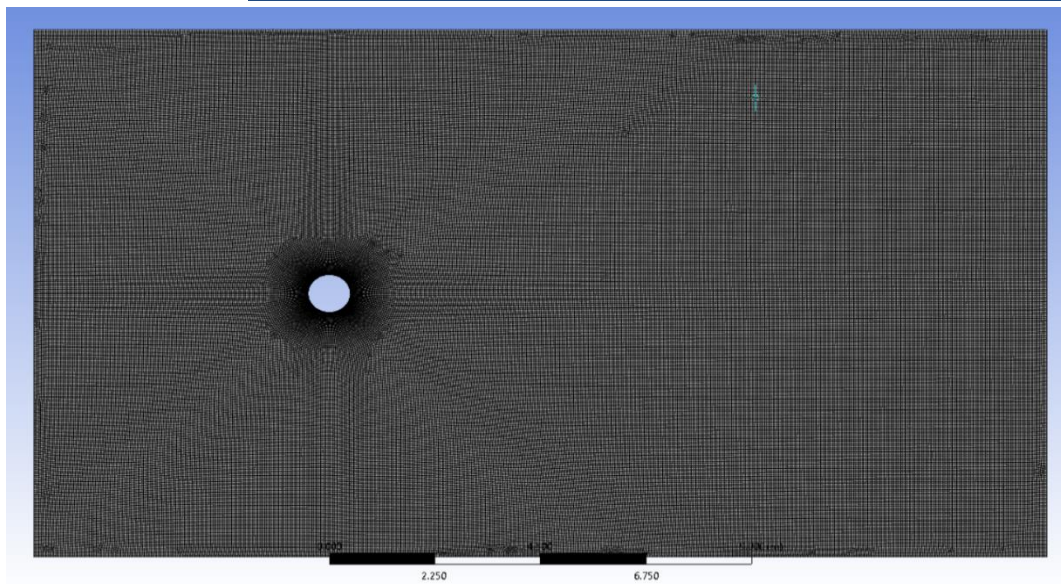


Fig 3.5: Meshing for the bare cylinder.

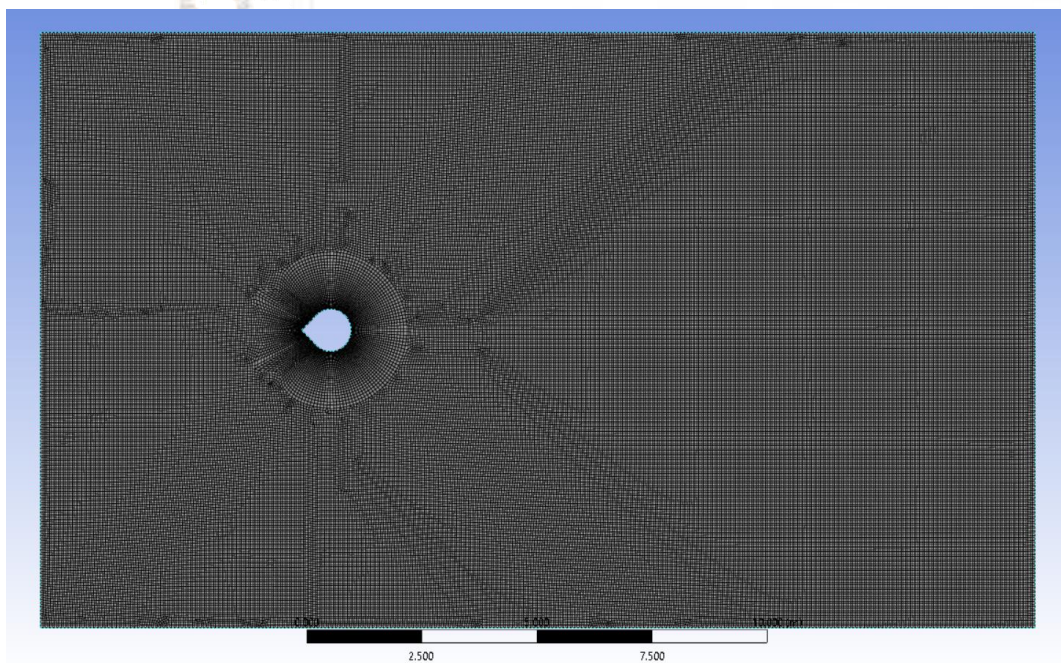


Fig 3.6: Meshing for the cylinder with fairing 0.125D

3.4 Computational Domain

Geometry parts are used only to define the faces, edges, and vertices that make up the surfaces of the model. The simulation domain on which mesh is generated, and for which physics is solved, is defined using regions, boundaries, and interfaces. An essential part of the process in setting up your simulation is therefore to define the relationship between geometry parts and regions, boundaries, and interfaces. The mesh continuum models cannot be used for geometry parts. In order to mesh geometry parts, they must be assigned to one or more regions, and the mesh is then generated for the region.

In this study seven different configuration for the conduits are made and its simulated for 2 different free stream velocities the computational domain for the configuration are explained below: -

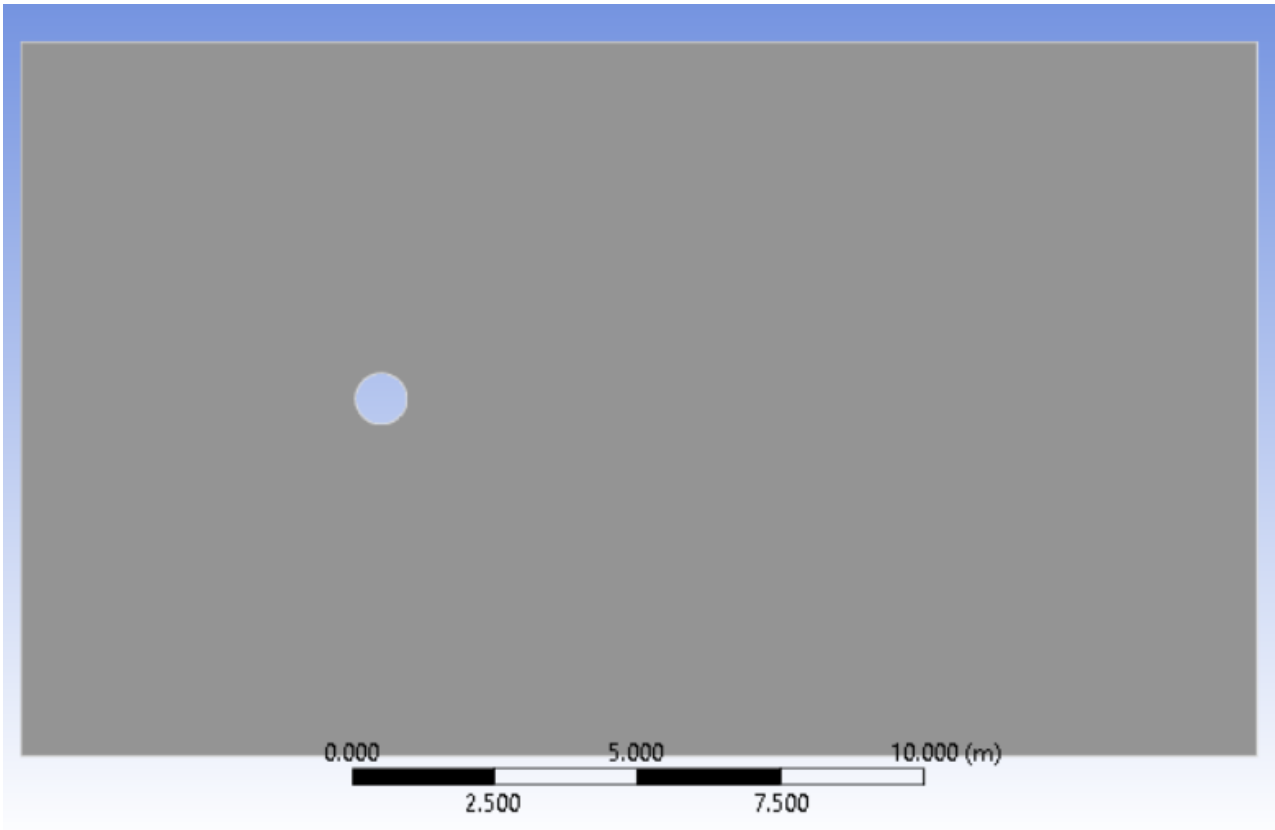
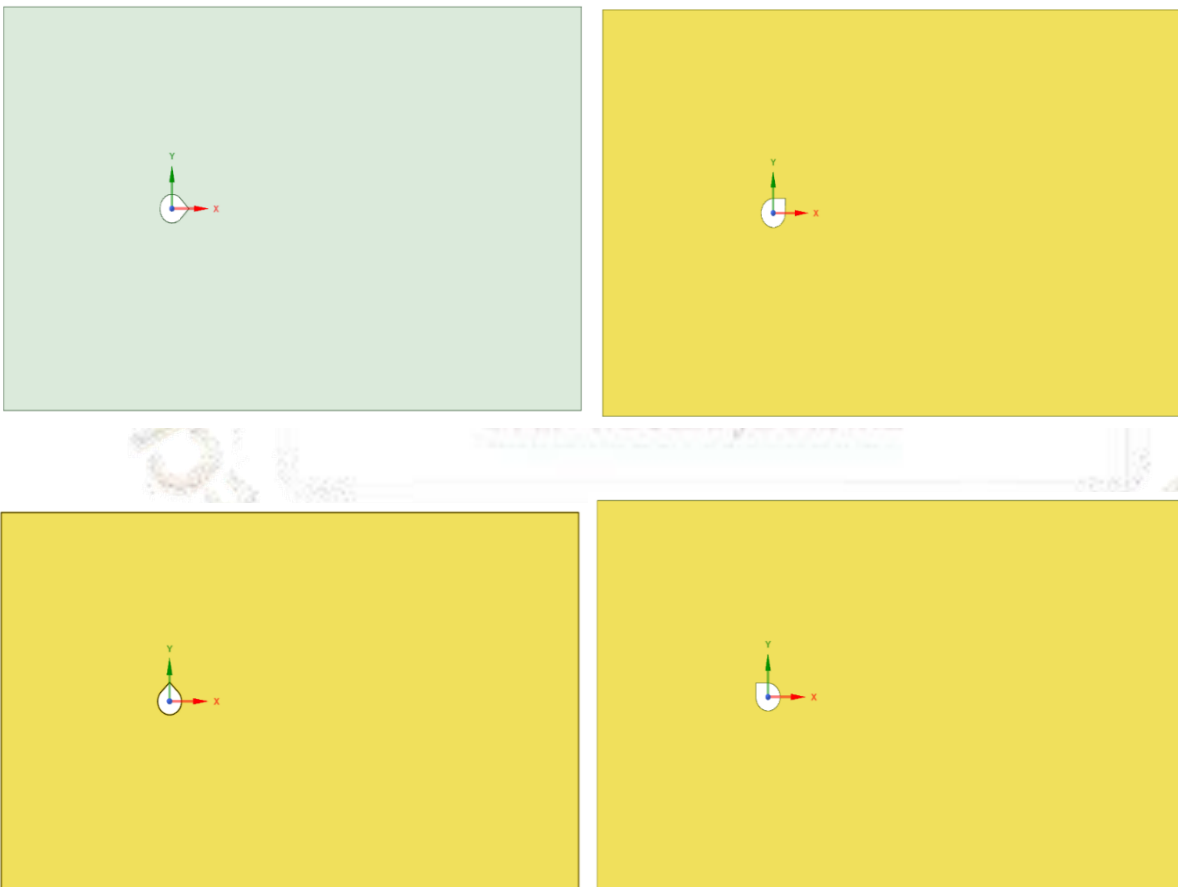


Fig 3.7: Domain configuration for the bare cylinder



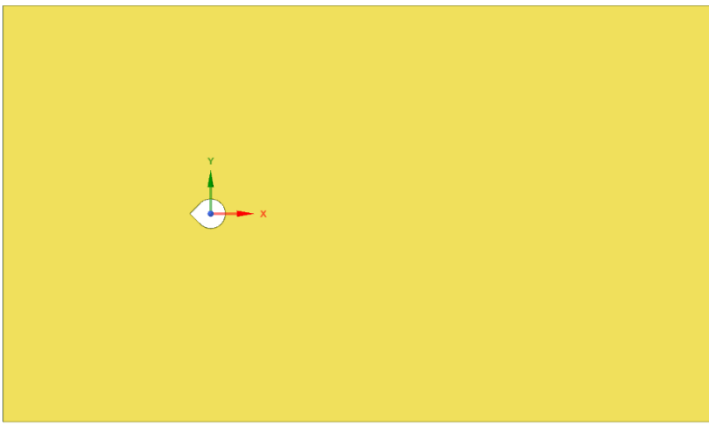


Fig 3.8: Domain configuration for cylinder with fairing 0.125D fixed at different angles.

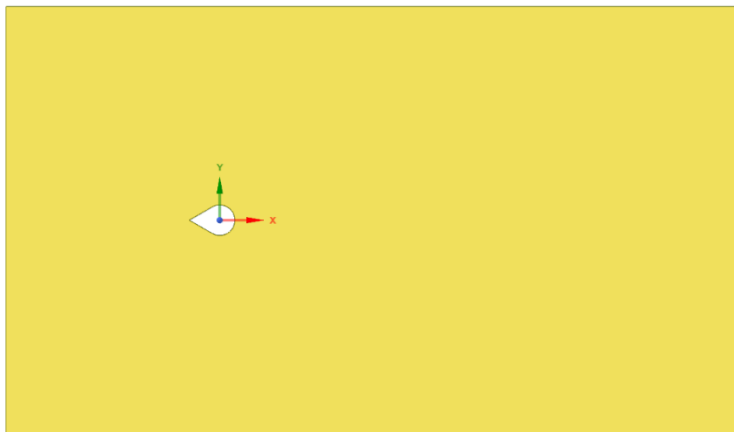


Fig 3.9: Domain configuration for the cylinder with fairing 0.25D at 180 degree.

3.5 BOUNDARY CONDITIONS

There are several boundary conditions for the discretized equations. Some of them which are used for this work are velocity inlet, pressure outlet, free slip wall, no slip wall.

Velocity Inlet

A velocity inlet boundary represents the inlet of a duct at which the flow velocity is known. It is applied for inlet to a simulation of incompressible internal flows. It can be used in combination with pressure outlet and flow split outlet boundaries.

Pressure Outlet

A pressure outlet boundary is a flow outlet boundary at which the pressure is specified. It can apply as an outflow of compressible and internal flows.

Wall

A wall boundary represents an impermeable surface. Applications of this boundary are as an impenetrable boundary for inviscid flows, as an impenetrable, no-slip boundary for viscous flow, “Slip walls” representing an impenetrable but traction-free surface.

Boundary Conditions Applied.

Inlet – velocity inlet.

Outlet- pressure outlet

Top and bottom – wall (free slip)

cylinder- wall (no slip)

3.6 PHYSICS MODELING

This chapter includes the details of physics models selected, solver setup, and stopping criteria. This chapter also includes details of spring model implemented. Calculation of Eigen frequency of spar still water using free decay test, flow velocities corresponding to the reduced velocities in lock in range is explained.

Physics models

The physics model in ANSYS FLUENT defines how a physical phenomenon in a continuum is represented. Essentially, physics models define the primary variables of the simulation (such as pressure, temperature, and velocity) and what mathematical formulation is used to generate the solution. Models in ANSYS FLUENT have varying levels of complexity and functionality but their major purpose are to work with solvers to obtain a solution. Both background region and overset region are provided with the same physics continuum. Table 2 gives the physics models selected.

Table 2 Physics Model

Material	Liquid water
Time	Implicit unsteady
Flow	Segregated flow
Viscous regime	turbulent
Turbulence model	Reynolds Averaged Navier Stokes (RANS)

3.6.1 Material modeling

The material model is responsible for managing the material, that is, substance or substances, being simulated in the continuum. The material, in turn, is responsible for managing the various thermodynamic and transport properties relevant to that material and to the physical processes being modelled in the continuum. Here in our study the risers are subjected within the sea, so the material chosen here is seawater and the properties are mentioned in the below table.

Table 3 Material Properties of Fluid

Material	Density	Dynamic Viscosity
water	1025kg/m ³	8.887E-4 Pa-s

3.6.2 Solution Methods

The Coupled Flow and Coupled Energy models are best for compressible flows, natural convection problems, and flows with large body forces or energy sources. The Segregated Flow model is an alternative for incompressible or mildly compressible flows, particularly when computational resources are an issue; it is used with the Segregated Fluid Energy models. For complex time-periodic flows, you can use Harmonic Balance Flow and Energy. In this study materials water and air are both provided considered as incompressible to reduce computational time. So, the segregated flow model is selected which is suitable for incompressible or mildly compressible flows. The Segregated Flow model solves the flow equations (one for each component of velocity, and one for pressure) in a segregated, uncoupled, manner. The linkage between the momentum and continuity equations is achieved with a predictor-corrector approach. A flow that is in a state of continuous instability, exhibiting irregular, small-scale, high frequency fluctuations in both space and time is termed turbulent. In this simulation since turbulent flow is encountered, turbulent flow viscous regime is selected. And the turbulence model selected is wale sub grid scale large eddy simulation model.

3.6.3 Modelling time

The Implicit Unsteady model is the only unsteady model available with the Segregated Flow and Segregated Fluid Energy models. It uses the Implicit Unsteady solver. Since segregated flow model is selected, implicit unsteady model is selected.

3.7 SOLVERS

Solvers control the solution and are activated once per iteration (or once per time-step for explicit unsteady simulations). Typically, a model elects the solvers that are required. Different models can use the same solver and sometimes models need more than one solver. Some models control other models and some only perform tasks when the solution is initialized. For this reason, not all models elect solvers. Models can also elect solvers that perform subsidiary tasks in addition to the solver that the model elected to control it. The following solvers have been used in this study.

3.7.1 Solver Parameter

In order to solve the present problem certain parameters need to be fixed so that computational grid can be solved effectively to achieve an approximate solution to the real problem. The solver parameters used in the present investigation is listed in Table.

Table 4 Solver parameters

Parameters	Adopted solver settings
Solver	Implicit unsteady
Velocity formulation	Absolute
Viscous Model	k-omega SST model
Operational Pressure	101325 PA
Gravitational Constant	981 m/s ²
Water Density	1024 kg/m ³
Water Viscosity	0.0010kg/m-s
Inlet boundary condition	Velocity inlet
Cylinder surface boundary condition	Wall (no slip)
Outlet boundary condition	Pressure outlet

Implicit unsteady solver

The Implicit Unsteady solver becomes active when the Implicit Unsteady model is active. Its primary function is to control the update at each physical time for the calculation. It also controls the time-step size.

CHAPTER 4 RESULTS AND DISCUSSION

4.1 General

This chapter deals with the discussion about the results of the Numerical simulations performed for bare cylinder and cylinder with fairings at different angles for different current speed.

4.2 CFD Results for the fairings arrangement

4.2.1 Bare Cylinder

Case 1). Current speed = 0.25 m/s

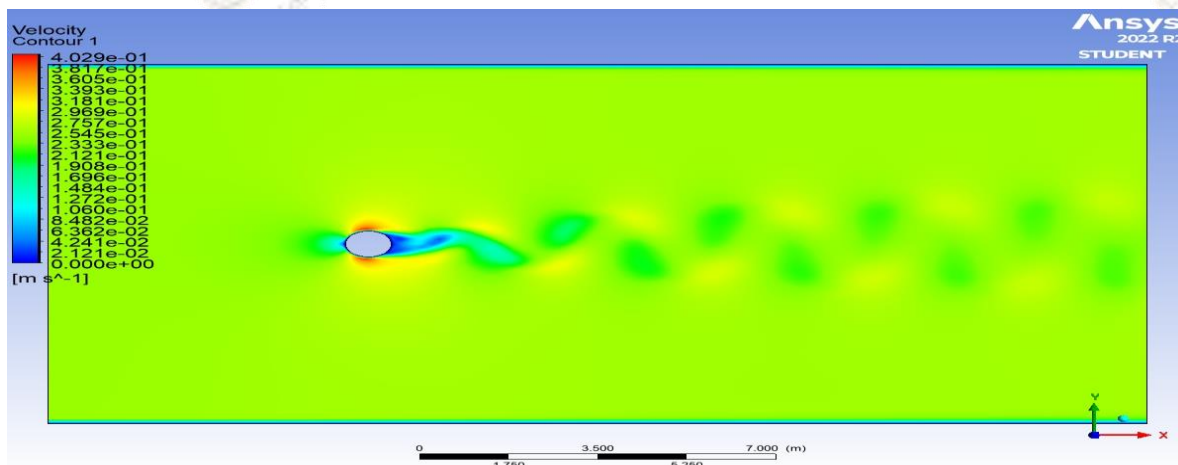


Fig 4.1: Bare cylinder velocity Contours for 0.25 m/s

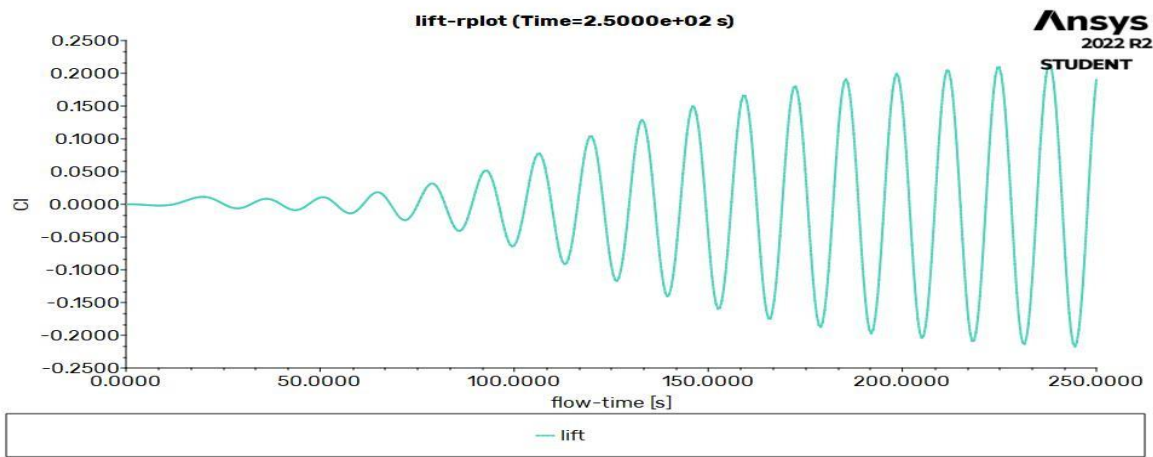


Fig 4.2: Bare cylinder Coefficient of lift v/s flowtime for 0.25m/s

Case 2). Current speed = 0.5m/s

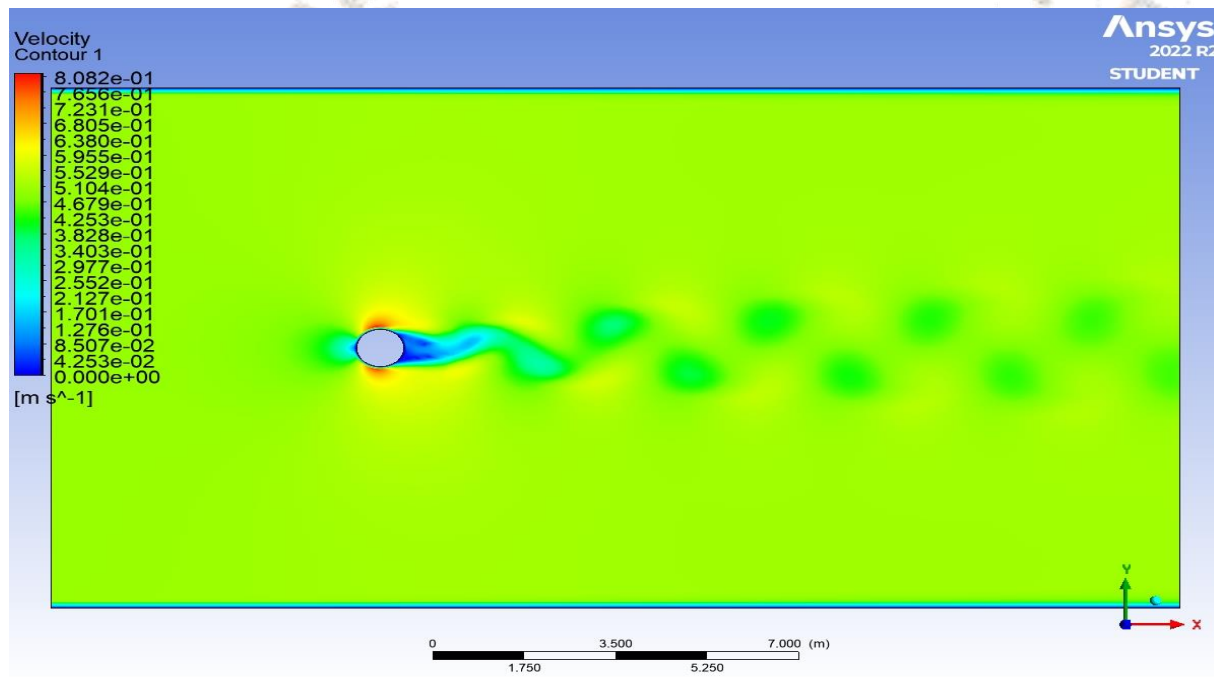


Fig 4.3: Bare cylinder Velocity contours for 0.5m/s

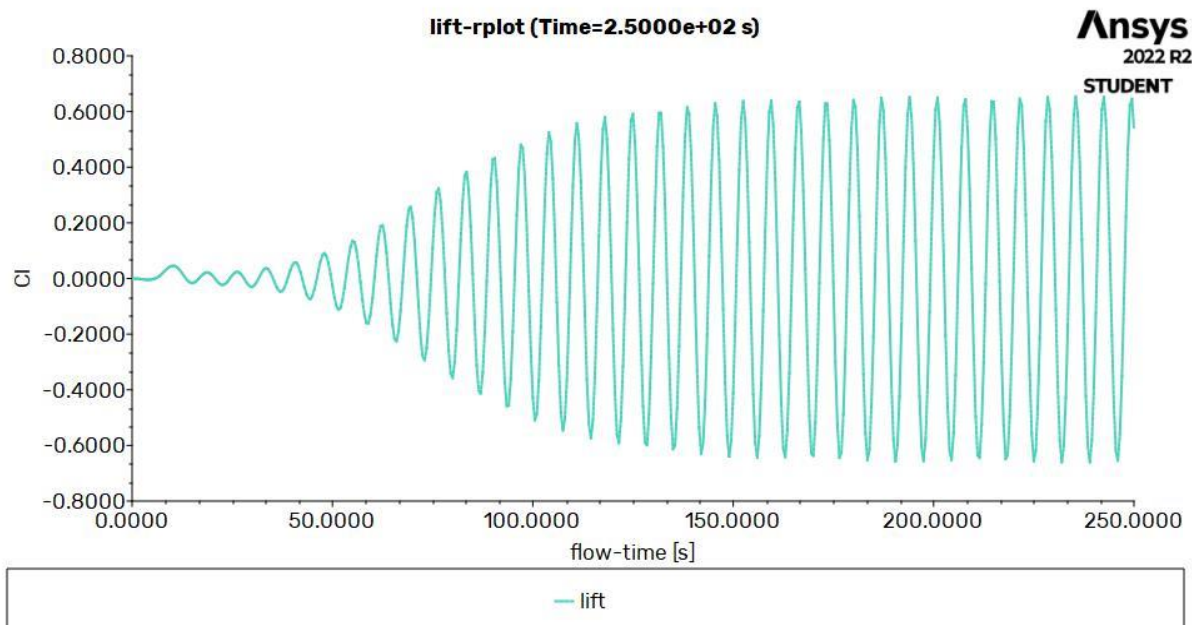


Fig 4.4: Bare cylinder Coefficient of lift v/s flowtime for 0.5m/s

4.2.2 Cylinder with fairing of 0.125D at an angle of Zero degree.

Case 1). Current speed = 0.25m/s

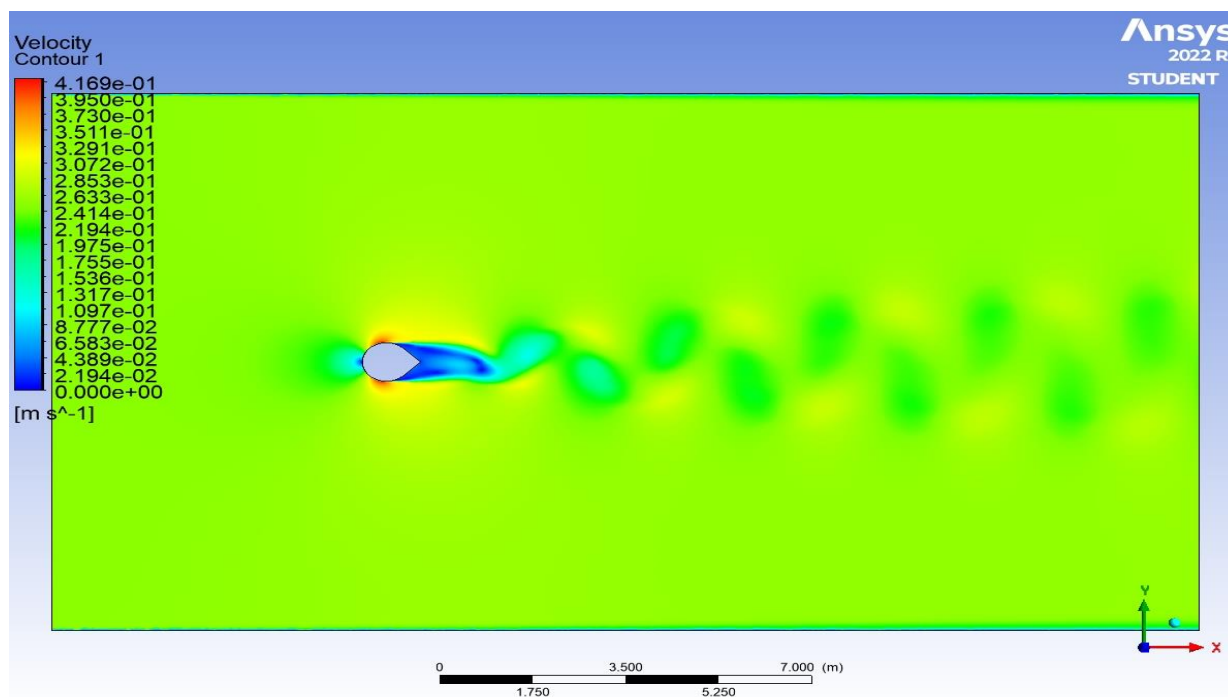


Fig 4.5: Velocity contours for cyl with fairing 0.125D at an angle of zero degree for 0.25m/s CS

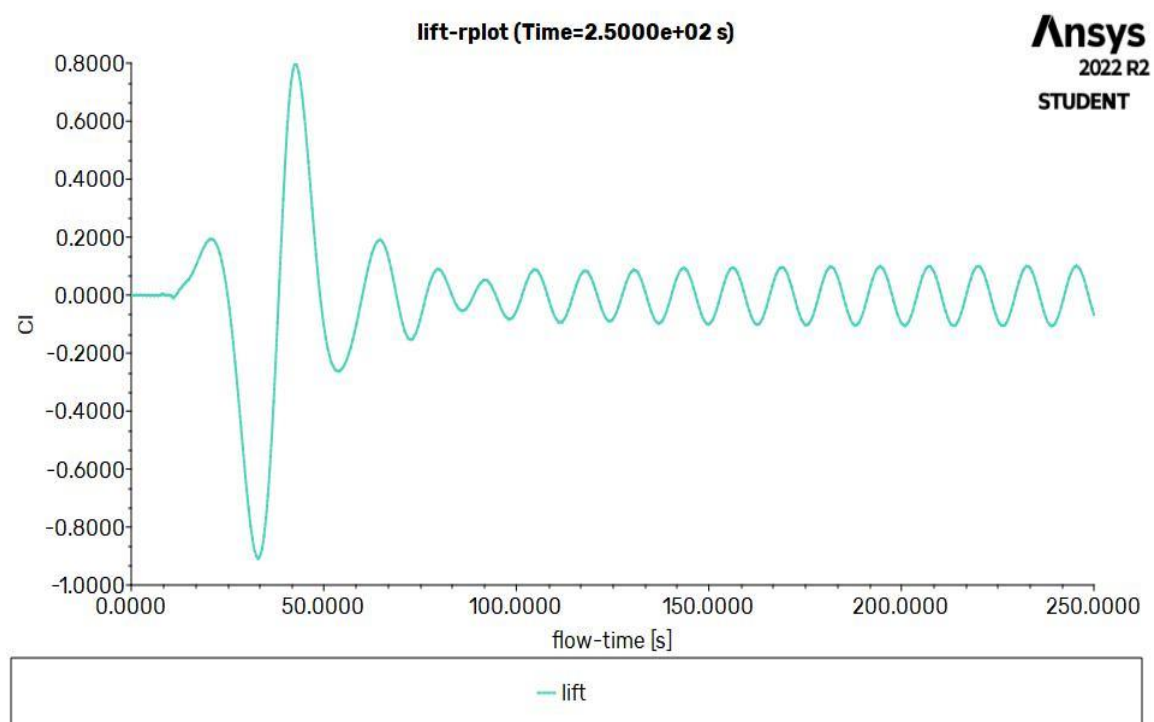


Fig 4.6: Coefficient of lift v/s flowtime for cyl with fairing 0.125D at an angle of zero degree for 0.25m/s CS

Case 2). Current speed = 0.5m/s

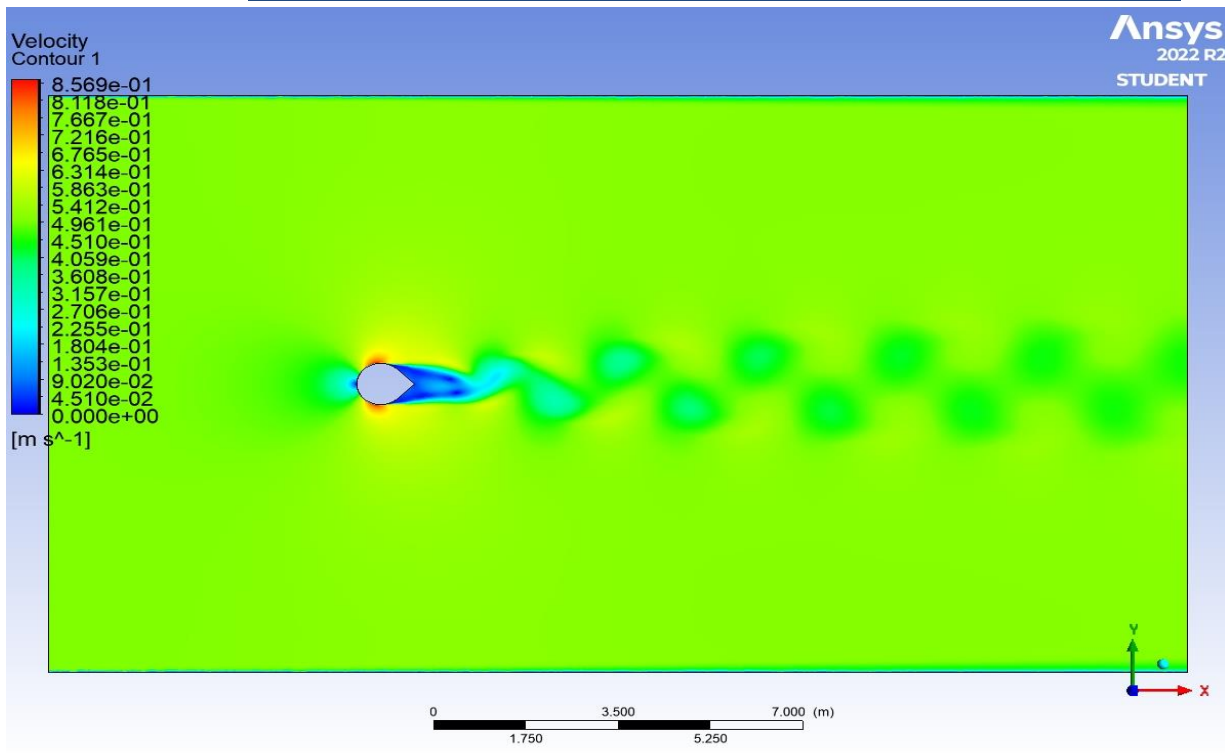


Fig 4.7: Velocity contours for cyl with fairing 0.125D at an angle of zero degree for 0.5m/s CS

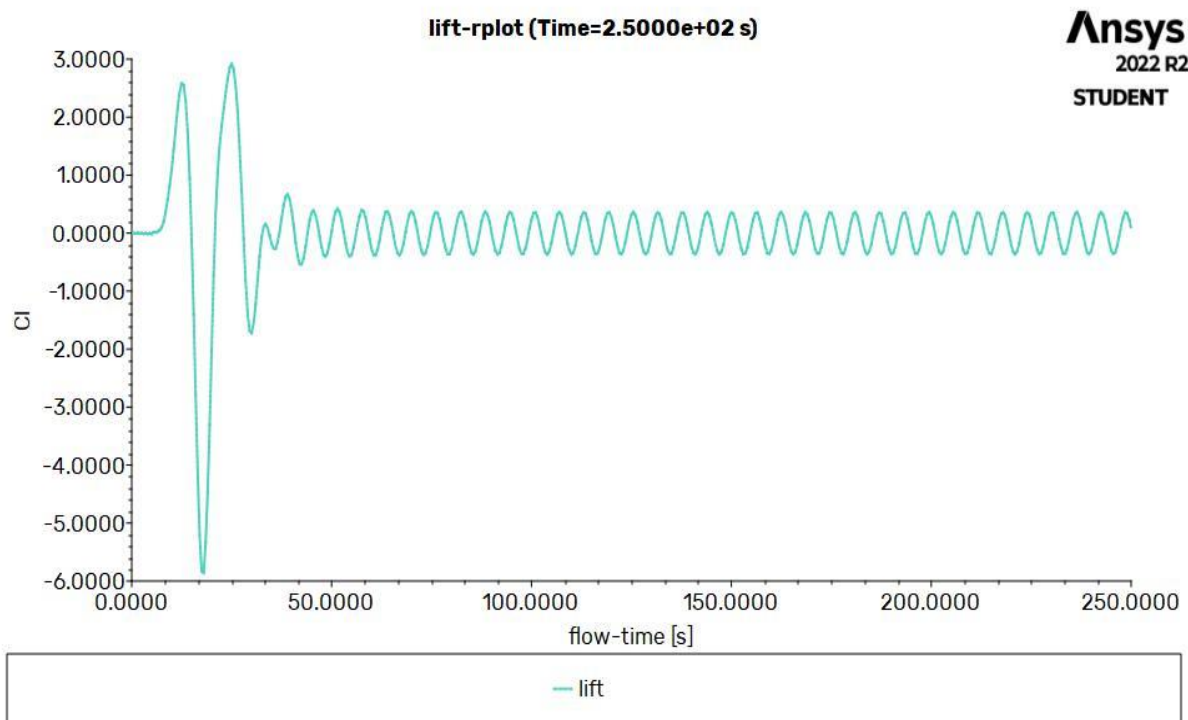


Fig 4.8: Coefficient of lift v/s flowtime for cyl with fairing 0.125D at an angle of zero degree for 0.5m/s CS

4.2.3 Cylinder with Fairing of 0.125D fixed at an angle of 45 degree.

Case 1). Current speed = 0.25m/s

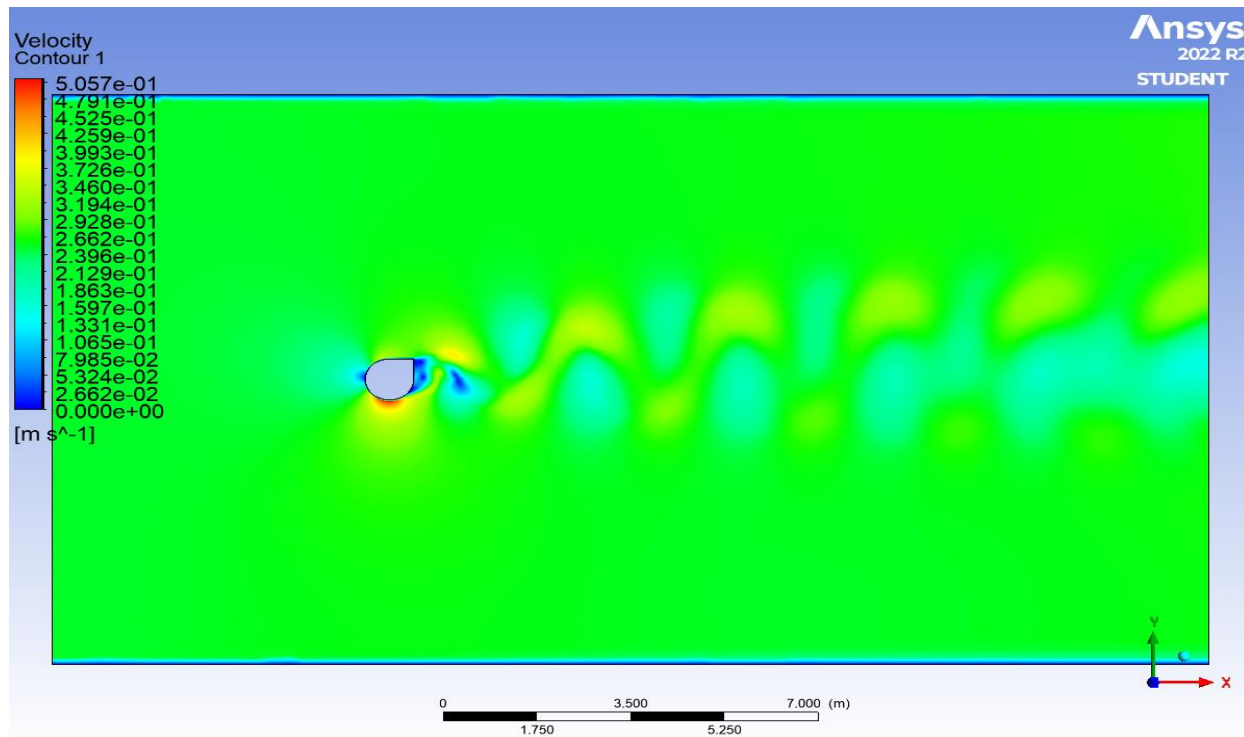


Fig 4.9: Velocity Contours for cyl with fairing 0.125D at an angle of zero degree for 0.25m/s CS

lift-rplot

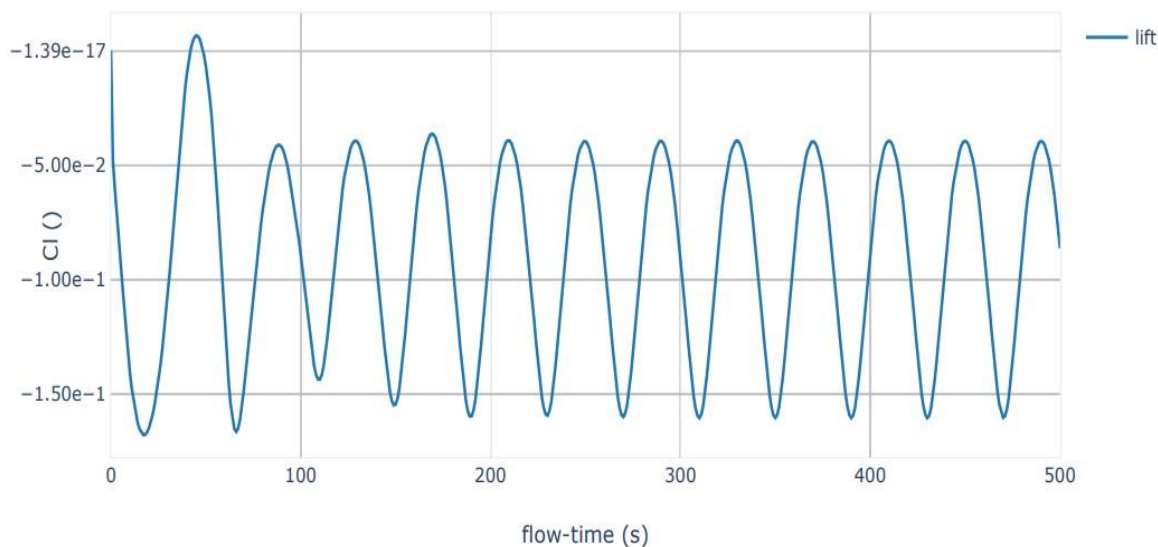


Fig 4.10: coefficient of lift v/s flowtime for cyl with fairing 0.125D at an angle of zero degree for 0.25m/s CS

Case 2). Current speed = 0.5 m/s

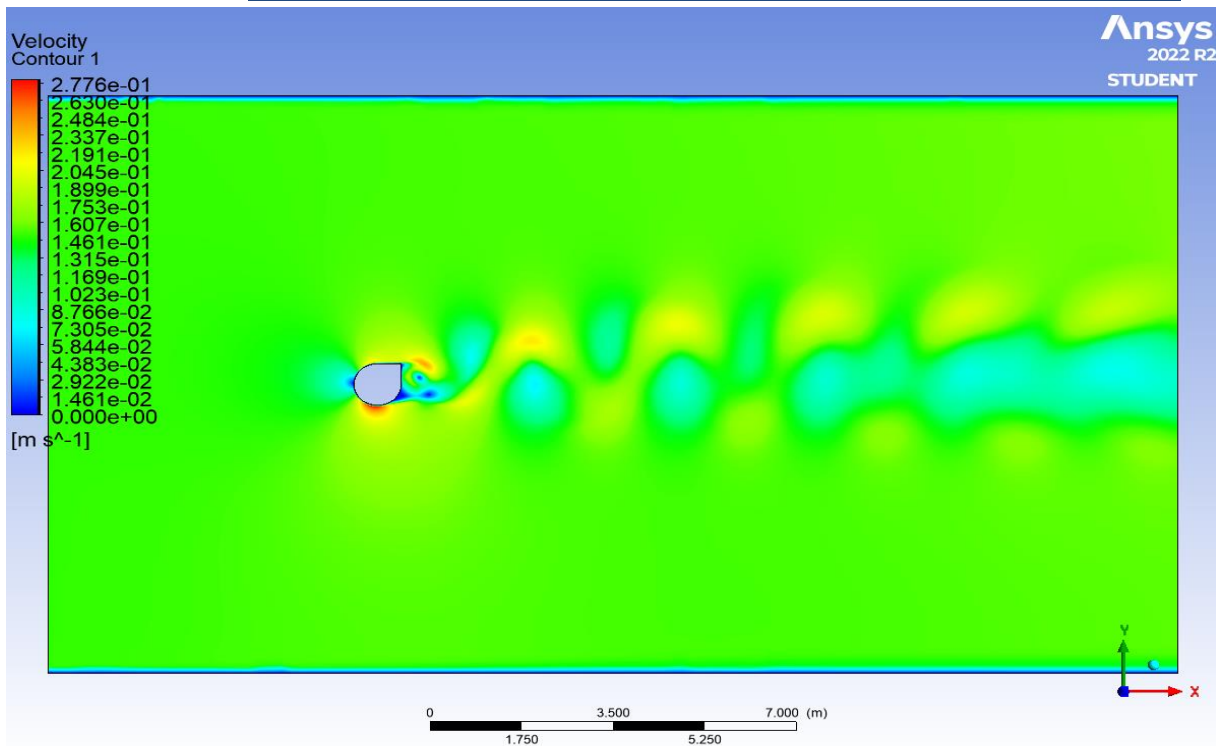


Fig 4.11: Velocity contours for cyl with fairing 0.125D at an angle of zero degree for 0.5m/s CS

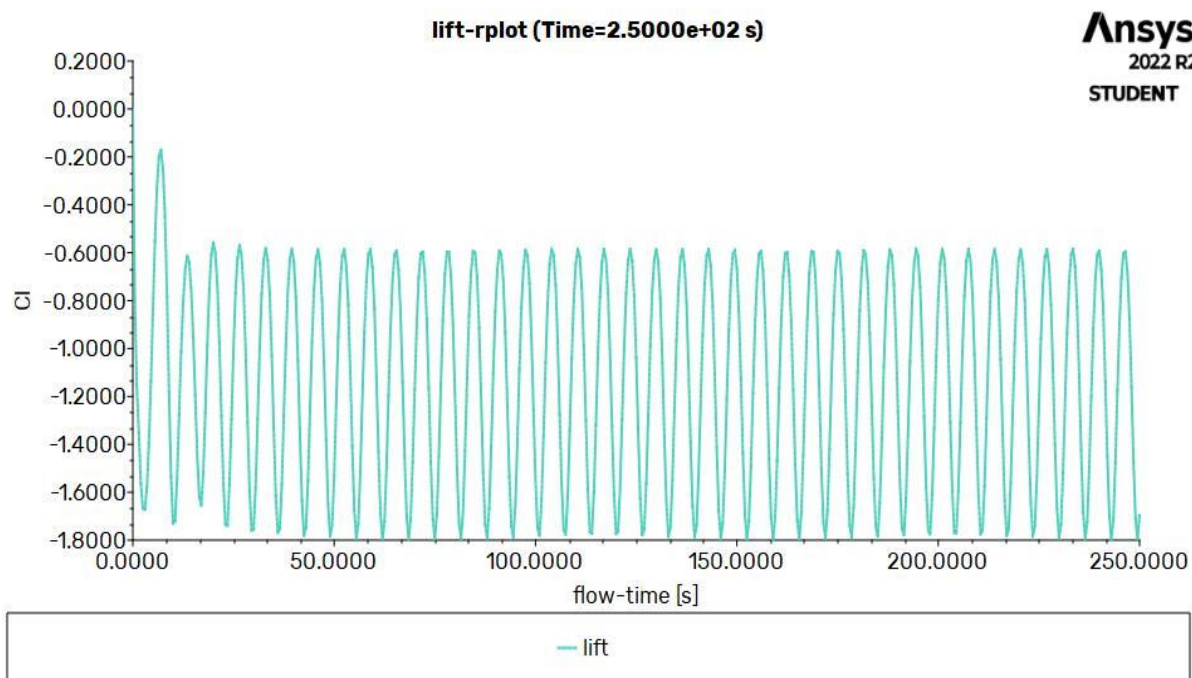


Fig 4.12: Coefficient of lift v/s flowtime cyl with fairing 0.125D at an angle of zero degree for 0.5m/s CS

4.2.4 Cylinder with Fairing of 0.125D fixed at an angle of 90 degree.

Case 1). Current speed = 0.25m/s

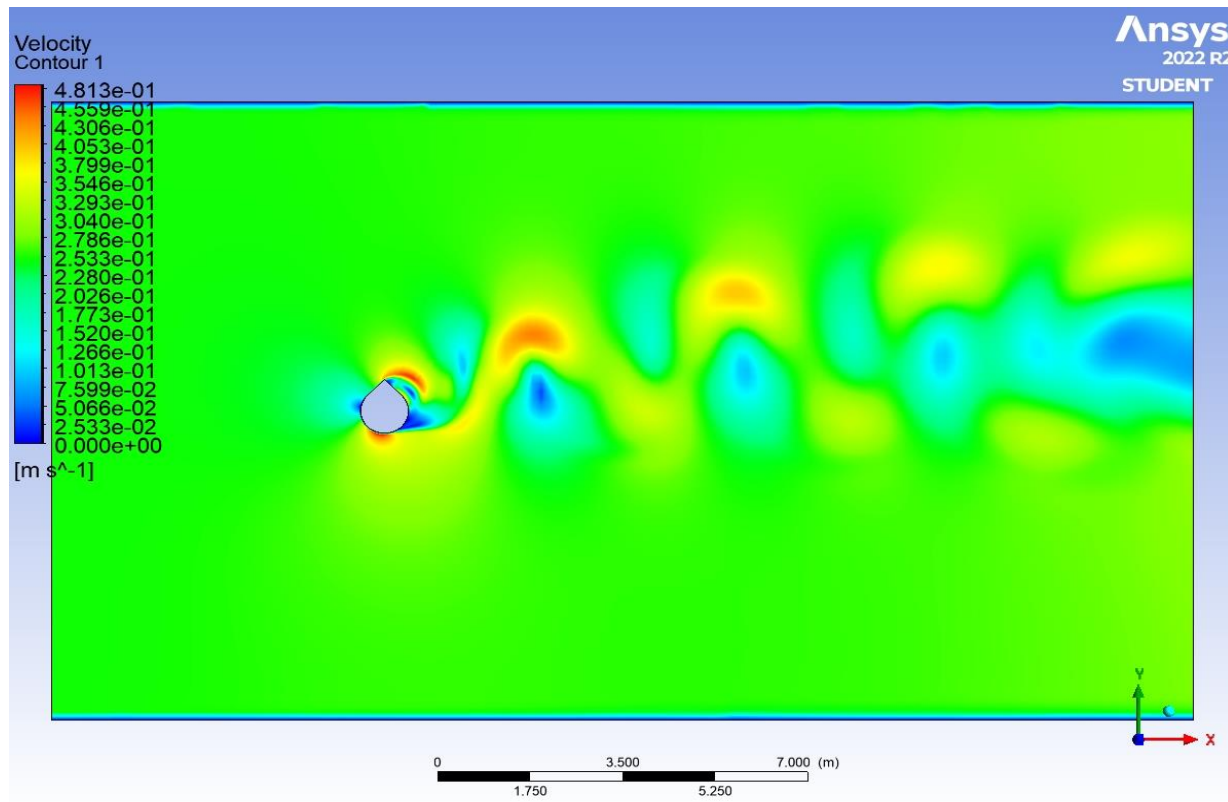


Fig 4.13: Velocity contours for cyl with fairing 0.125D at an angle of zero degree for 0.25m/s CS

lift-rplot

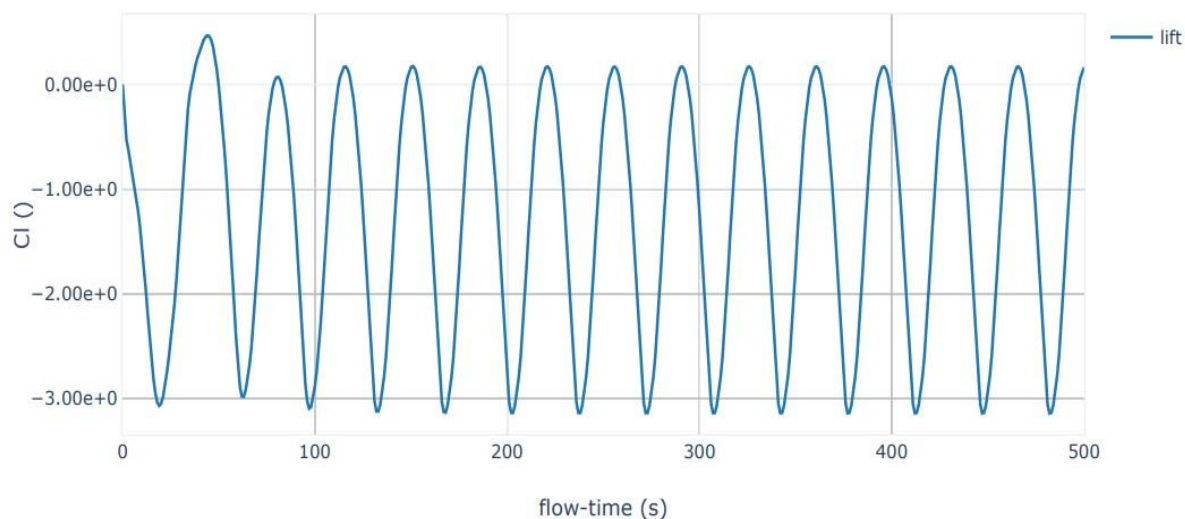


Fig 4.14: Coefficient of lift v/s flowtime for cyl with fairing 0.125D at an angle of zero degree for 0.25m/s CS

Case 2). Current speed = 0.5m/s

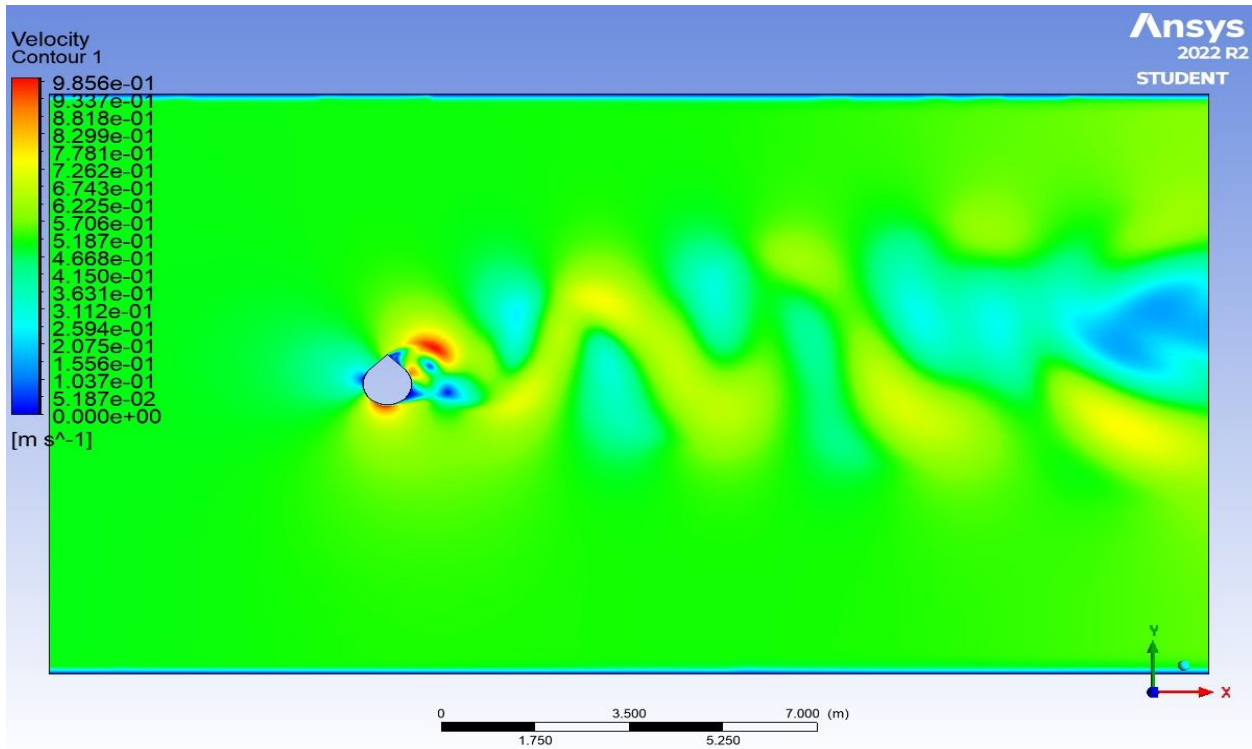


Fig 4.15: Velocity contours for cyl with fairing 0.125D at an angle of zero degree for 0.5m/s CS

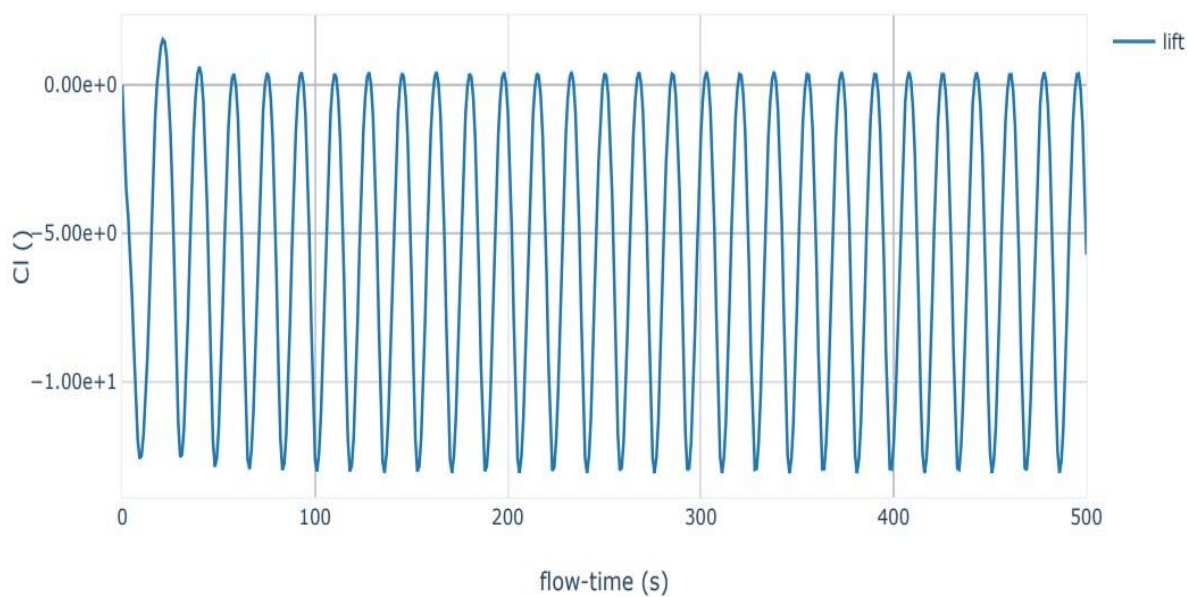


Fig 4.16: Coefficient of lift v/s flowtime for cyl with fairing 0.125D at an angle of zero degree for 0.5m/s CS

4.2.5 The cylinder with fairing of 0.125D fixed at an angle of 135 degree.

Case 1). Current speed = 0.25m/s

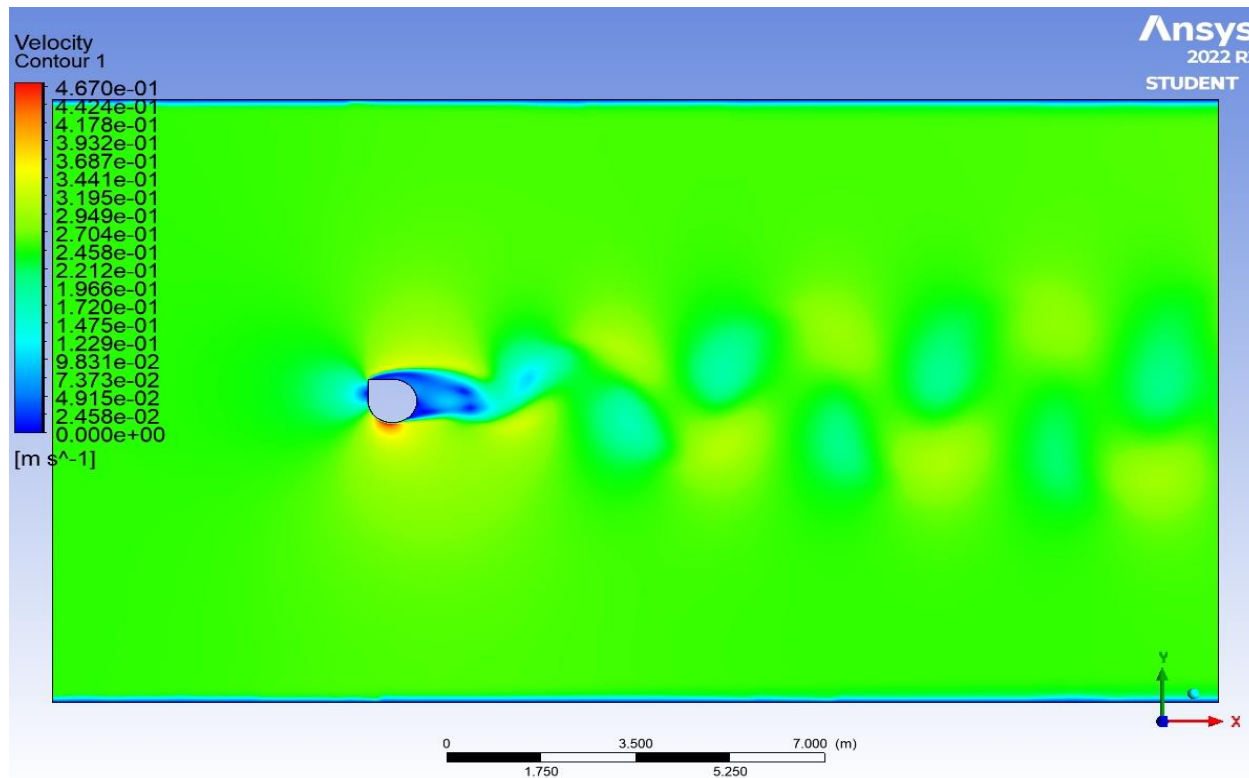


Fig 4.17: Velocity contours for cyl with fairing 0.125D at an angle of zero degree for 0.25m/s CS

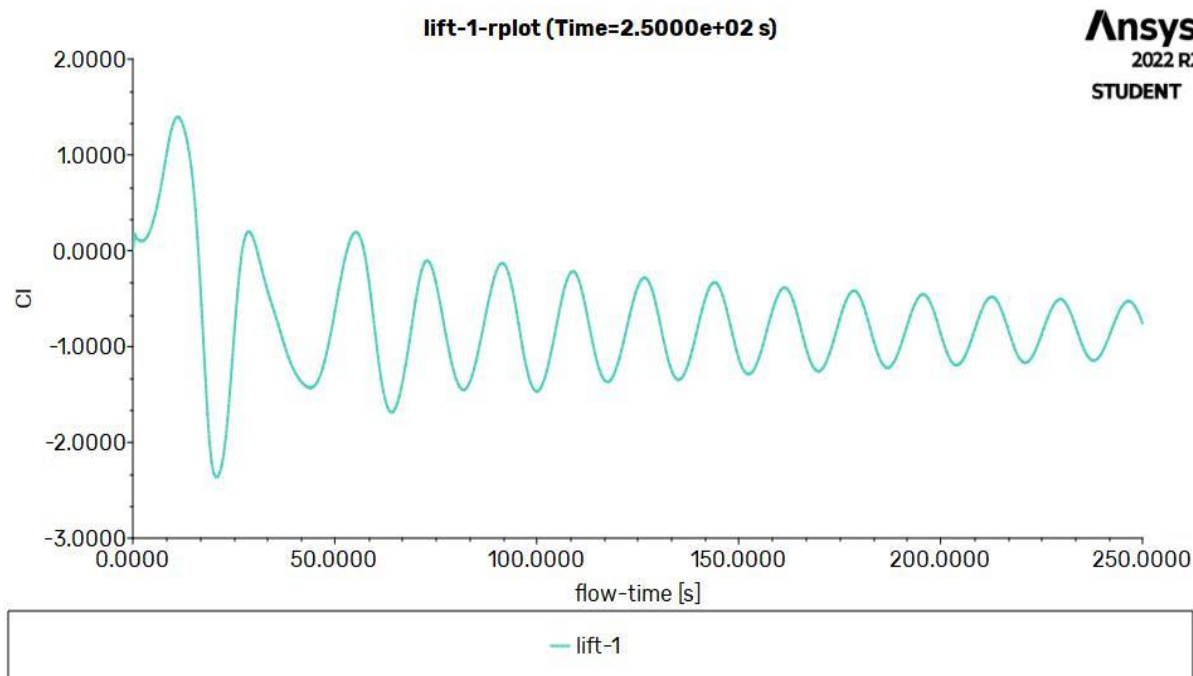


Fig 4.18: Coefficient of lift v/s flowtime for cyl with fairing 0.125D at an angle of zero degree for 0.25m/s CS

Case 2). Current speed = 0.5m/s

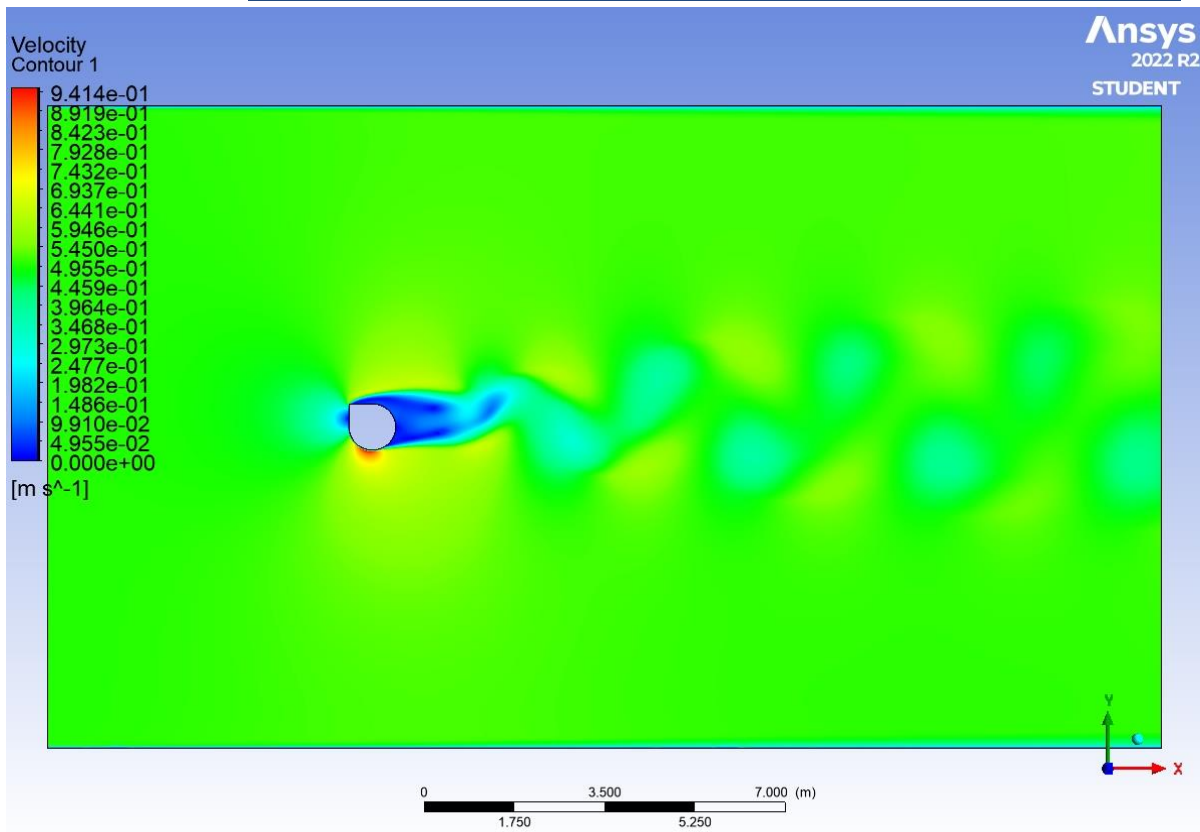


Fig 4.19: Velocity contours for cyl with fairing 0.125D at an angle of zero degree for 0.5m/s CS

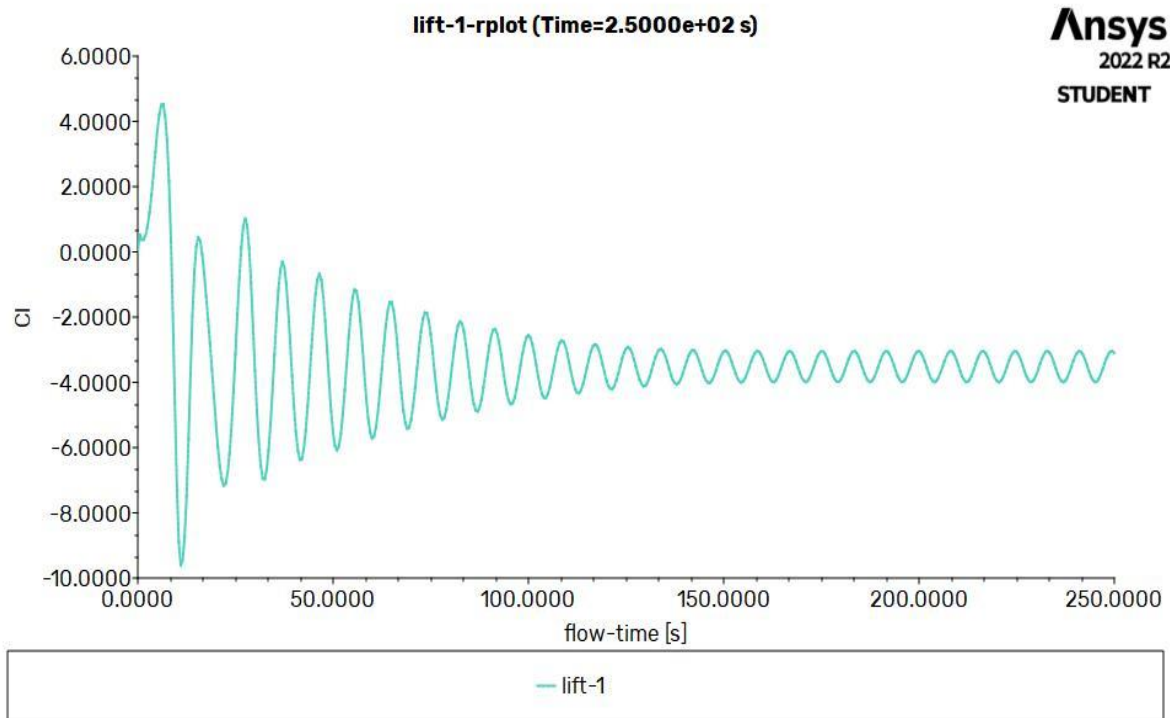


Fig 4.20: Coefficient of lift v/s flowtime for cyl with fairing 0.125D at an angle of zero degree for 0.5m/s CS

4.2.6 The cylinder with fairing of 0.125D fixed at an angle of 180 degree.

Case 1). Current speed = 0.25m/s

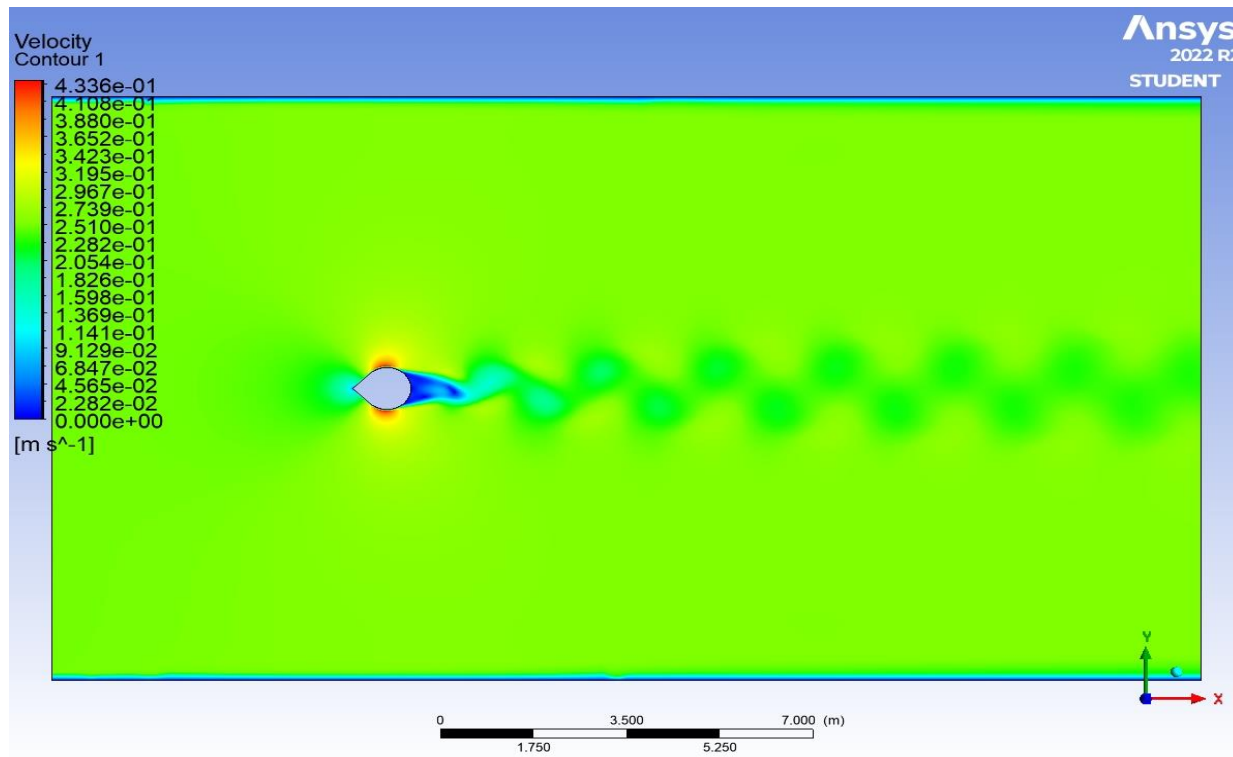


Fig 4.21: Velocity Contours for cyl with fairing 0.125D at an angle of zero degree for 0.25m/s CS

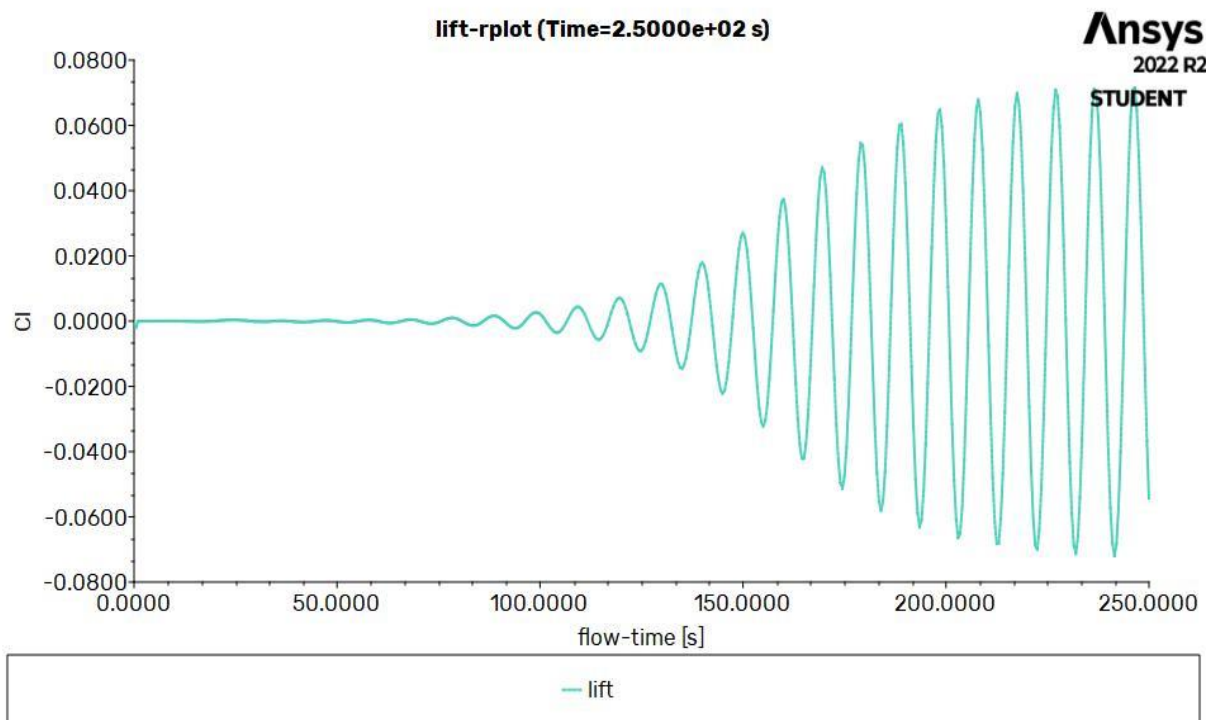


Fig 4.22: Coefficient of lift v/s flowtime for cyl with fairing 0.125D at an angle of zero degree for 0.25m/s CS

Case 2). Current speed = 0.5m/s

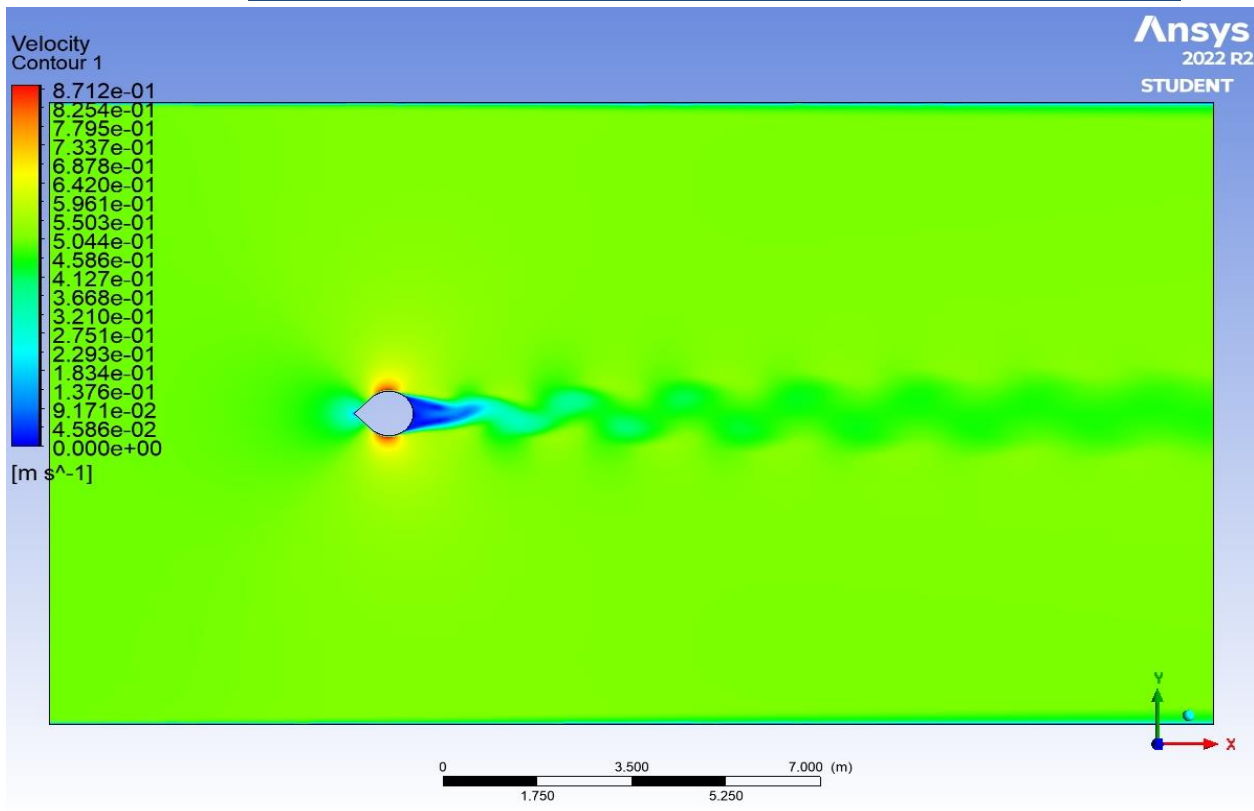


Fig 4.23: Velocity contours for cyl with fairing 0.125D at an angle of zero degree for 0.5m/s CS

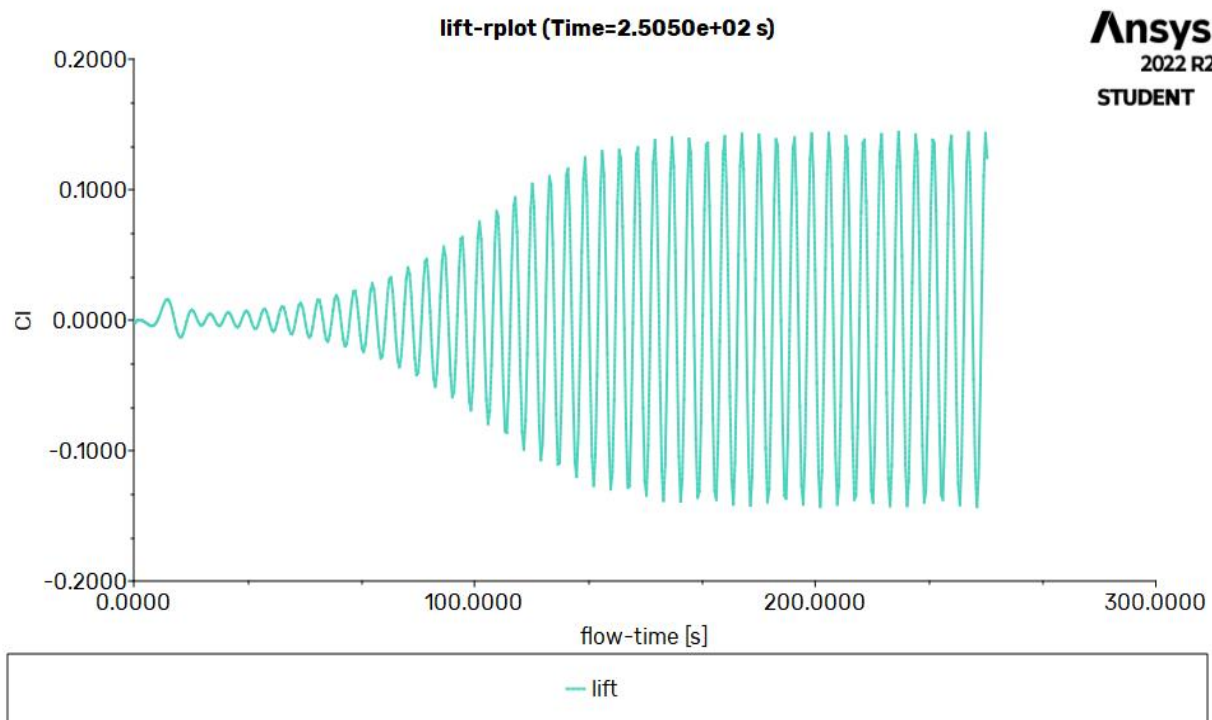


Fig 4.24: Coefficient of lift v/s flowtime for cyl with fairing 0.125D at an angle of zero degree for 0.5m/s CS

4.2.7 The Cylinder with fairing of 0.25D fixed at an angle of 180 degree.

Case 1). Current speed = 0.25m/s

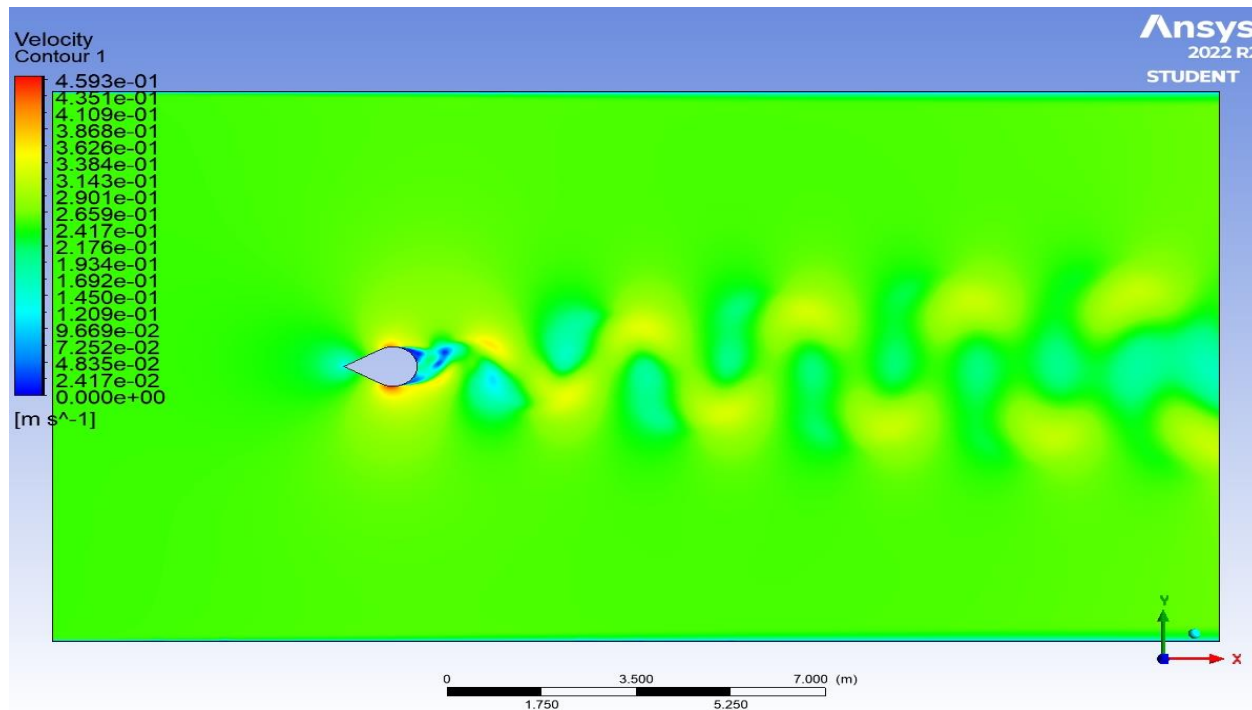


Fig 4.25: Velocity contours for cyl with fairing 0.25D at an angle of zero degree for 0.25m/s CS

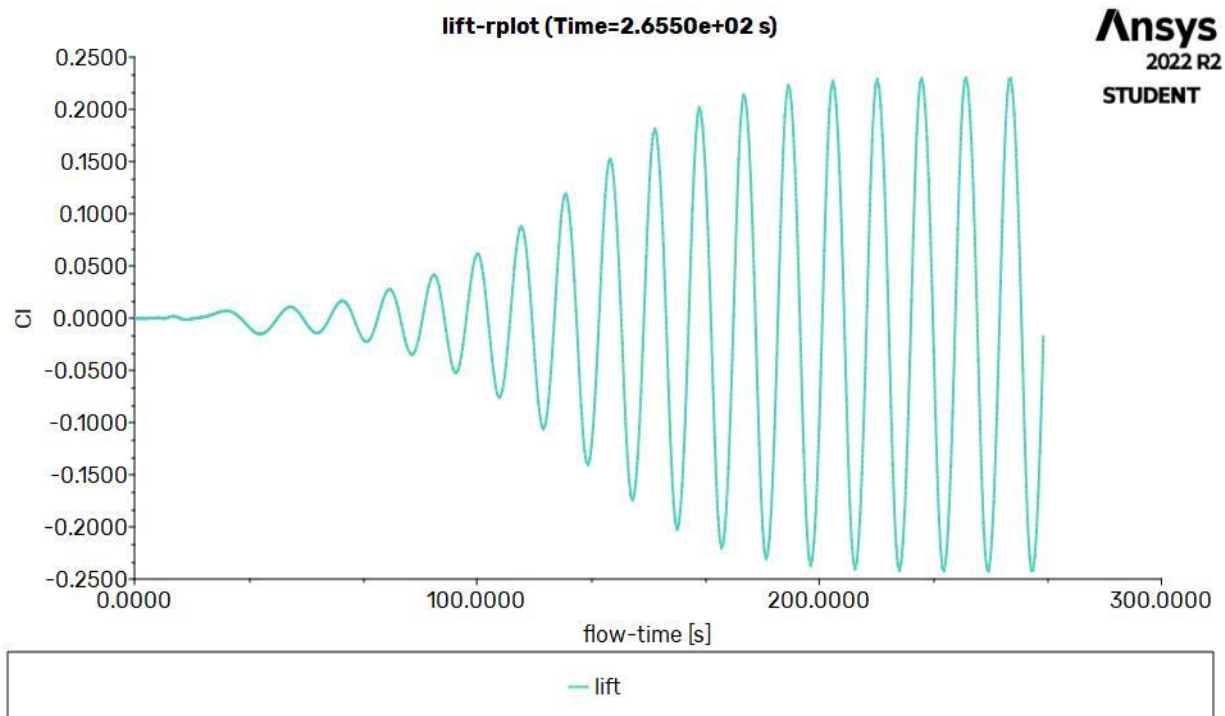


Fig 4.26: Coefficient of lift v/s flowtime cyl with fairing 0.25D at an angle of zero degree for 0.25m/s CS

Case 2). Current speed = 0.5m/s

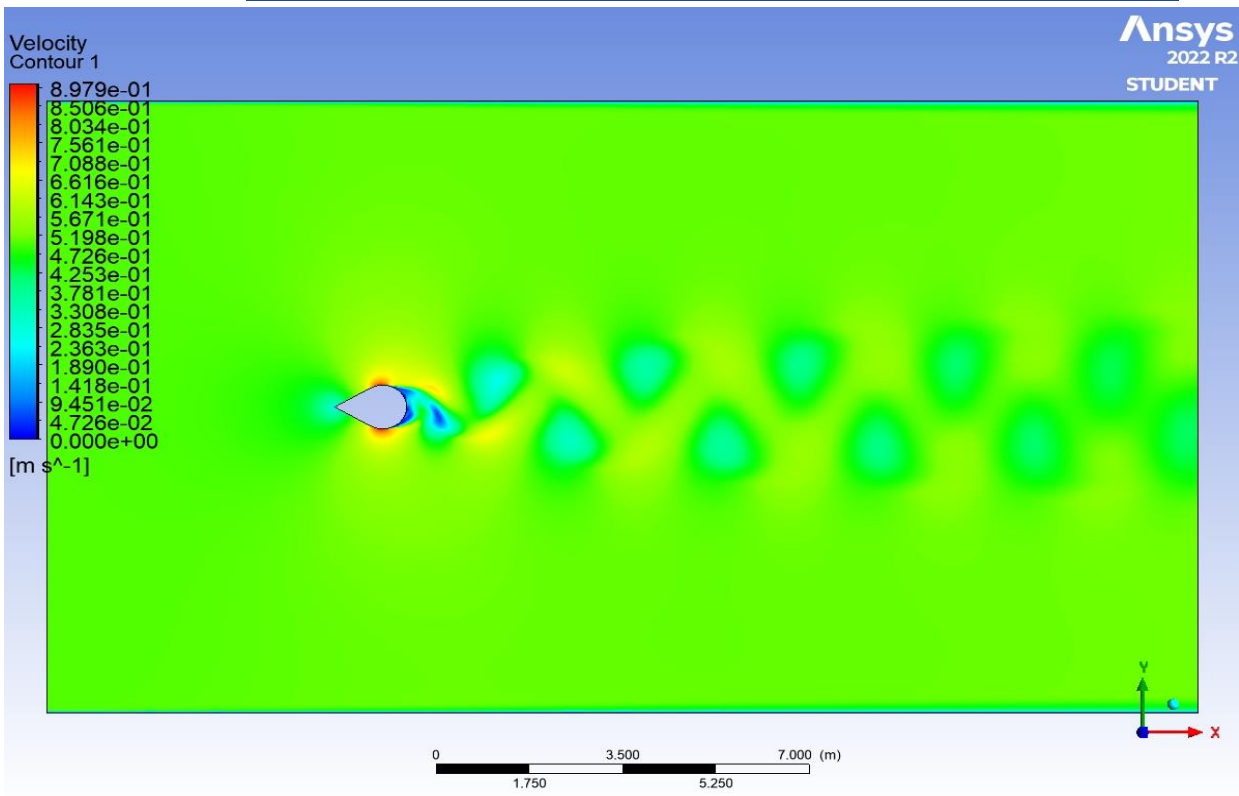


Fig 4.27: Velocity contours for cyl with fairing 0.25D at an angle of zero degree for 0.5m/s CS

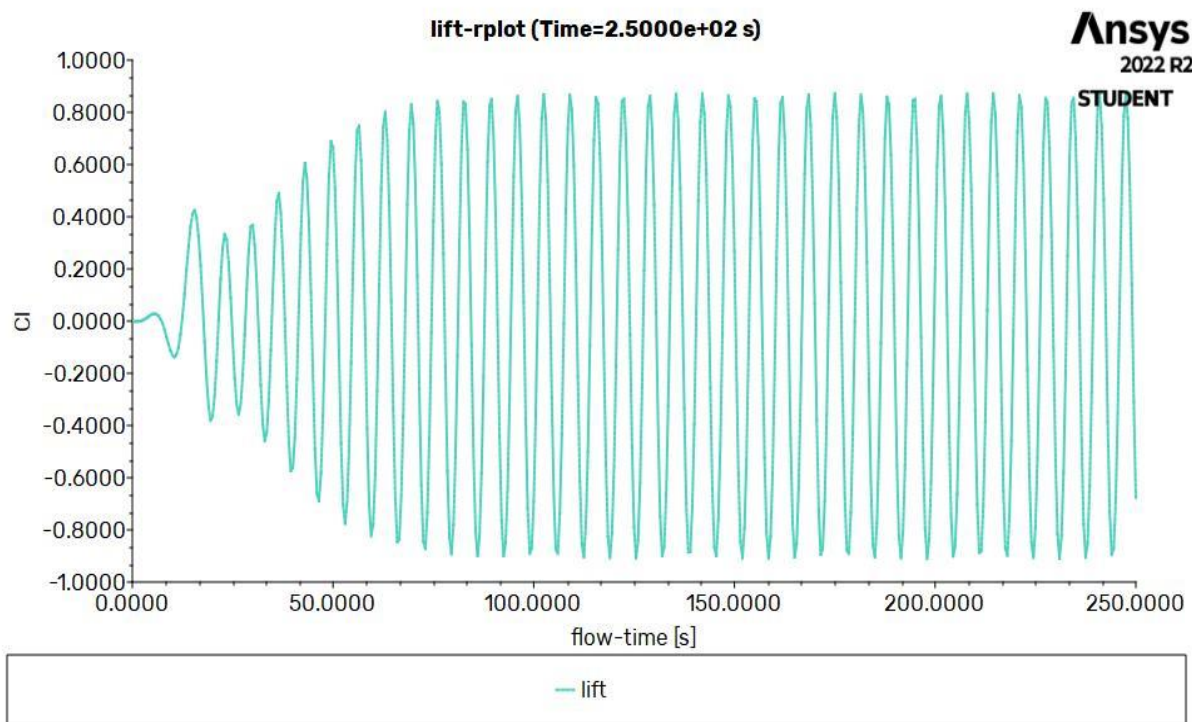


Fig 4.28: Coefficient of lift v/s flowtime cyl with fairing 0.25D at an angle of zero degree for 0.5m/s CS

RESULT TABLE

Table No.5 List of obtained coefficient of lift values.

Sl. No.	Type of cylinder	Angle	Current speed (m/s)	Lift Coefficient (Cl)
01	Bare	-	0.25	0.1913959
02	Bare	-	0.5	0.5372883
03	With 0.125D fairing	Zero	0.25	-0.0675923
04	With 0.125D fairing	Zero	0.5	1.450176e-27≈0
05	With 0.125D fairing	45°	0.25	-1.866447
06	With 0.125D fairing	45°	0.5	-0.0684217
07	With 0.125D fairing	90°	0.25	0.1640284
08	With 0.125D fairing	90°	0.5	-5.723619
09	With 0.125D fairing	135°	0.25	-0.7536188
10	With 0.125D fairing	135°	0.5	-3.105413
11	With 0.125D fairing	180°	0.25	-0.05476332
12	With 0.125D fairing	180°	0.5	0.1240201
13	With 0.25D fairing	180°	0.25	-0.01796491
14	With 0.25D fairing	180°	0.5	-0.6813356

CHAPTER 5**SUMMARY AND CONCLUSIONS****5.1 Summary**

In this thesis, numerical simulations of flow past circular conduits were carried out at different free stream velocities for different arrangement of cylinder with fairings fixed at different angles. ANSYS FLUENT was used for this study as a solver for the study. Simulation was carried out over a flow past a circular conduit for two different current speeds. In these different configurations of the conduits the effect of the presence of one another was analysed such as lift variation over time over the domain.

5.2 Conclusions

The salient conclusions from the study are as follows:

1. It has been observed that for most cases the values of lift force is higher in case of the bare cylinders in comparison with the results for cylinder arrangement with attached fairing.
2. It has been observed that the lift force is increased for bare cylinder as we increase the current speed.
3. It has been observed that the vortex induced vibrations are reduced and lift force is decreased after attaching the fairings to the cylinder.
4. The trial has been done for two types of fairings i.e., fairing of 0.125D and fairing of 0.25D.
5. Thus, by the analysis conducted we can conclude that for cylinder with fairing 0.125D fixed at an angle of 0° for the current speed 0.5m/s the coefficient of lift is more or less it's equal to Zero (0).

REFERENCES

1. Xiaojian Jin, Shunqi Yang , Hai Chen (2017) Research on Fairing design and CFD Analysis of Submarine Pipeline Inspection ARV, MATEC Web of Conferences 108, 07003.
2. Syamsul Azry Md Esa, Wan Mohd. Arif Aziz Japar, Nor Azwadi Che Sidik (2019) Design and Analysis of Vortex Induced Vibration (VIV) Suppression Device, Akademia baru ISSN: 2180-1363.
3. Nursahliza Binti Muhamat Yain (2017) Marine riser Vortex Induced Vibration (VIV) suppression Device.
4. Syazwan Bin Sazali (2016) Vortex induced vibration (VIV) reduction measure on dimpled concrete coated pipeline.
5. Satya Prakash Singh, Gautam Biswas, Perumal Nithiarasu (2013) A numerical study of vortex shedding from a circular cylinder vibrating in the in-line direction, DOI: 10.1108/HFF-08-2012-0183.
6. Meghanadhan C A, Sunil A S (2016) An Experimental Study of Vortex Shedding Behind a Bluff Body in a Water Channel, (IJERT) ISSN: 2278-0181.
7. Alok Mishra, Ashoke De, Suppression of vortex shedding using a slit through the circular cylinder at low Reynolds number.
8. Aswin Janardhanan (2014) Reducing Vortex-Induced Vibration of Drilling Risers with Marine Fairing, Spring 5-16-2014.